Supporting Information

Multicomponent reaction-based discovery of pyrimido[2,1-*b*][1,3]benzothiazole (PBT) as a novel core for full-color-tunable AIEgens

Shan-Shan Gong,[ab‡] Rui Kong,[b‡] Chunhong Zheng,[b] Congbin Fan,[b] Chengjun Wang,[b] Dong-Zhao Yang,[b] Zhen-Zhen Chen,[b] Shuwang Duo,[b] Shouzhi Pu*[abc], and Qi Sun*[b]

[a]*College of Chemistry, Nanchang University, 999 Xuefu Avenue, Nanchang, Jiangxi 330031, PR China*

[b]*Jiangxi Key Laboratory of Organic Chemistry, Jiangxi Science and Technology Normal University, 605 Fenglin Avenue, Nanchang, Jiangxi 330013, PR China*

[c]*Department of Ecology and environment, Yuzhang Normal University, Nanchang, Jiangxi 330103, PR China*

[‡]*The authors contributed equally to this work.*

E-mails: pushouzhi@tsinghua.org.cn; sunqi@jxstnu.edu.cn

Table of contents

1. General methods

1.1 Synthesis of PBT compounds

All chemical reagents and solvents were obtained from commercial suppliers. All reactions were performed in commercial AR grade solvents without inert gas protection and monitored by thin layer chromatography on plates coated with 0.25 mm silica gel 60 F_{254}. TLC plates were visualized by UV irradiation (254 nm and 365 nm). Flash column chromatography employed silica gel (particle size 32–63 μm). N MR spectra were obtained with a Bruker AV-400 instrument with chemical shifts reported in parts per million (ppm, δ) and referenced to $CDCl_3$, MeOH-d_4, or DMSO-d_6. IR spectra were recorded on a Bruker Vertex-70 spectrometer. Low-resolution and high-resolution mass spectra were obtained with a Bruker amaZon SL mass spectrometer and a Bruker Dalton micrOTOF-Q II spectrometer, respectively, and reported as *m*/*z*. Melting points were determined with a Thomas-Hoover melting point apparatus and uncorrected.

1.2 UV-Vis and fluorescence spectrometry

Absorption spectra of solution samples ([PBT]=1×10^{-5} M) were recorded on an Aglient 8453 spectrophotometer. Absorption spectra of solid samples were recorded on a PerkinElmer Lambda 750 spectrophotometer. Fluorescence spectra of solution ([PBT]=5×10^{-5} M) and solid samples were recorded on a Hitachi F-4600 fluorescence spectrophotometer. Optical length of the quartz cell was 10 mm. Fluorescence quantum yields of solution ([PBT]=5×10^{-5} M) and solid samples were determined on a Hamamatsu absolute PL quantum yield spectrometer C11347. Fluorescence lifetimes were recorded on a Hamamatsu compact fluorescence lifetime spectrometer C11367.

1.3 Theoretical calculations

Ground-state geometrical optimization of PBT molecules were carried out at the B3LYP/6-31G(d) level of theory implemented on the Gaussian 09 or 16 package. Selected parameters for the vertical excitation of **PBT-1**, **PBT-A4**, **PBT-AB1**, and **PBT-BC3** in THF were obtained by TD–DFT calculations at the identical level of theory.

The quantitative correlation of the rotation of the ester and the distortion of pyrimidine ring was calculated by using def2-SVP basis set. The ground state and excited state geometries with the ester twisted for 0º, 90º, 270º, and 360º were optimized through PCM(THF)-PBE0 method.

1.4 DLS measurement

Particle size distribution was measured on a Nano Brook 90 Plus instrument equipped with a diode laser as a light source (λ = 640.0 nm). The scattered light from the sample solution was detected using a fixed angle (90°).

1.5 SEM measurement

Scanning electron microscopy (SEM) was conducted on a Zeiss Sigma field emission scanning electron microscope. The suspension of **PBT-A2** ([PBT]=2×10^{-5} M) in dioxane–water mixture (f_w = 95 vol%) was immediately frozen in liquid nitrogen and lyophilized under vacuum. The sample powder was deposited onto a silicon wafer and coated with Au under a vacuum using ion sputtering before measurement. The SEM measurement was performed under an accelerating voltage of 10.0 kV.

1.6 X-ray crystallographic analysis

Data collection for X-ray crystal analysis was performed on a Bruker Smart APEX-II single

crystal X-ray diffractometer using graphite monochromated Mo-Kα radiation (λ = 0.71073 Å) at 296 K. The single crystals of PBT compounds obtained by recrystallization from specific solvent system as mentioned in the Section 2.3. The structures were solved by direct methods using SHELXL crystallographic software package. Crystallographic data are available from the Supporting Information (Section 6) or the Cambridge Crystallographic Data Centre (CCDC): No. 2082831, 2083529, and 2083668–2083684.

2. Synthetic procedures and characterization data of PBT compounds

2.1 General procedure for the 3CR synthesis of PBT-1, PBT-As, B1–B4, Cs, D1, and AB1

To a mixture of aldehyde (1.2 eq.), β-ketoester/diketone (1.5 eq.), and 2-aminobenzo- thiazole/2-aminobenzoxazole (1.0 eq.) was added $Hf(OTf)_4$ (0.01 eq.). The reaction was stirred in a sealed reaction tube at 80 °C for 2–24 h. Flash column chromatography of the crude reaction mixture afforded the target PBT compounds in pure form.

2.2 General procedure for the synthesis of PBT-BC1–BC3

To a solution of **PBT-B1** (1.0 mmol) and benzaldehyde or substituted benzylaldehydes (4.0 mmol) in ethanol (10 mL) was added KOH (2.5 mmol). The reaction was stirred at room temperature for 1–4 h and concentrated *in vacuo*. Flash column chromatography afforded **PBT-BCs** in pure form.

2.3 Characterization data of PBT compounds

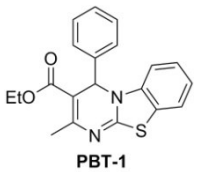

PBT-1

Ethyl 2-methyl-4-(phenyl)-4*H*-pyrimido[2,1-*b*][1,3]benzothiazole-3-carboxylate (PBT-1). The reaction of benzaldehyde (127 mg, 1.2 mmol), ethyl acetoacetate (195 mg, 1.5 mmol), 2-aminobenzothiazole (150 mg, 1.0 mmol), and $Hf(OTf)_4$ (8 mg, 0.01 mmol) followed by flash column chromatography (PE/EA=10:1) afforded **PBT-1** (315 mg, 90%) as a yellow solid; mp 189–190 °C. Single crystal was cultured by recrystallization from CH_2Cl_2/hexane. ^{1}H NMR (400 MHz, $CDCl_3$): δ 7.43–7.41 (m, 3H), 7.27–7.17 (m, 4H), 7.12–7.08 (m, 2H), 6.39 (s, 1H), 4.21–4.11 (m, 2H), 2.45 (s, 3H), 1.30–1.22 (m, 3H) ppm; ^{13}C NMR (100 MHz, $CDCl_3$): δ 166.7, 163.5, 154.9, 141.6, 138.2, 128.7 (×2), 128.4, 127.3 (×3), 126.7, 124.0, 122.2, 111.9, 103.2, 60.2, 57.9, 23.8, 14.5 ppm; IR (KBr): ν_{max} 3434, 2970, 1669, 1592, 1511, 1459, 1369, 1326, 1267, 1243, 1201, 1098, 746 cm^{-1}; LRMS (ESI+): *m/z* calcd for $C_{20}H_{19}N_2O_2S$ $[M+H]^+$ 351.1; found 351.1.

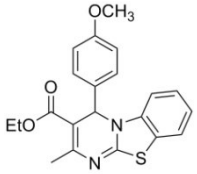

PBT-A1

Ethyl 2-methyl-4-(4-methoxyphenyl)-4*H*-pyrimido[2,1-*b*][1,3]benzothiazole-3-carboxylate (PBT-A1). The reaction of 4-methoxybenzaldehyde (163 mg, 1.2 mmol), ethyl acetoacetate (195 mg, 1.5 mmol), 2-aminobenzothiazole (150 mg, 1.0 mmol), and $Hf(OTf)_4$ (8 mg, 0.01 mmol) followed by flash column chromatography (PE/EA=10:1) afforded **PBT-A1** (312 mg, 82%) as a

yellow solid; mp 115–116 °C. Single crystal was cultured by recrystallization from CH_2Cl_2/hexane. ^{1}H NMR (400 MHz, $CDCl_3$): δ 7.43 (d, J=7.8 Hz, 1H), 7.35 (d, J=8.1 Hz, 2H), 7.24 (d, J=7.8 Hz, 1H), 7.20–7.05 (m, 2H), 6.77 (d, J=8.1 Hz, 2H), 6.34 (s, 1H), 4.20–4.11 (m, 2H), 3.72 (s, 3H), 2.45 (s, 3H), 1.28 (t, J=6.9 Hz, 3H) ppm; ^{13}C NMR (100 MHz, $CDCl_3$): δ 166.8, 163.4, 159.6, 154.7, 138.3, 134.0, 128.6 (×3), 126.7, 124.0, 122.3, 114.0 (×2), 111.9, 103.4, 60.2, 57.4, 55.3, 23.9, 14.5 ppm; IR (KBr): ν_{max} 3434, 2978, 1699, 1671, 1584, 1510, 1370, 1328, 1267, 1240, 1203, 1175, 1076, 1031, 978, 843, 744 cm^{-1}; LRMS (ESI+): *m/z* calcd for $C_{21}H_{21}N_2O_3S$ $[M+H]^+$ 381.1; found 381.1.

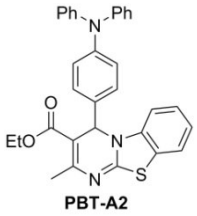

PBT-A2

Ethyl 2-methyl-4-(4-diphenylaminophenyl)-4*H*-pyrimido[2,1-*b*][1,3]benzothiazole-3-carboxylate (PBT-A2). The reaction of 4-diphenylaminobenzaldehyde (328 mg, 1.2 mmol), ethyl acetoacetate (195 mg, 1.5 mmol), 2-aminobenzothiazole (150 mg, 1.0 mmol), and $Hf(OTf)_4$ (8 mg, 0.01 mmol) followed by flash column chromatography (PE/EA=10:1) afforded **PBT-A2** (311 mg, 60%) as a yellow solid; mp 197–198 °C. ^{1}H NMR (400 MHz, $CDCl_3$): δ 7.44 (d, J=7.7 Hz, 1H), 7.28–7.16 (m, 7H), 7.14–7.11 (m, 2H), 7.01–6.96 (m, 6H), 6.88 (d, J=8.5 Hz, 2H), 6.32 (s, 1H), 4.23–4.12 (m, 2H), 2.44 (s, 3H), 1.27 (t, J=7.1 Hz, 3H) ppm; ^{13}C NMR (100 MHz, $CDCl_3$): δ 166.8, 163.4, 154.9, 147.9, 147.6, 138.4, 135.0, 129.4 (×4), 128.2 (×2), 126.7, 125.0 (×4), 124.1, 124.0, 123.4 (×3), 122.7 (×2), 122.3, 112.0, 103.3, 60.2, 57.4, 23.9, 14.6 ppm; IR (KBr): ν_{max} 3418, 3060, 3033, 2978, 2930, 1672, 1590, 1510, 1361, 1324, 1270, 1235, 1169, 1095, 840, 740 cm^{-1}; HRMS (ESI+): *m/z* calcd for $C_{32}H_{28}N_3O_2S$ $[M+H]^+$ 518.1897; found 518.1899.

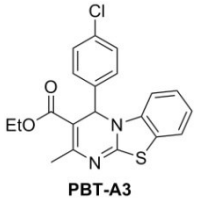

PBT-A3

Ethyl 2-methyl-4-(4-chlorophenyl)-4*H*-pyrimido[2,1-*b*][1,3]benzothiazole-3-carboxylate (PBT-A3). The reaction of 4-chlorobenzaldehyde (168 mg, 1.2 mmol), ethyl acetoacetate (195 mg, 1.5 mmol), 2-aminobenzothiazole (150 mg, 1.0 mmol), and $Hf(OTf)_4$ (8 mg, 0.01 mmol) followed by flash column chromatography (PE/EA=10:1) afforded **PBT-A3** (338 mg, 88%) as a yellow solid; mp 120–121 °C. Single crystal was cultured by recrystallization from CH_2Cl_2/hexane. ^{1}H NMR (400 MHz, $CDCl_3$): δ 7.43 (d, J=7.7 Hz, 1H), 7.36 (d, J=8.2 Hz, 2H), 7.24–7.20 (m, 3H), 7.13 (dd, J_1=J_2=7.7 Hz, 1H), 7.04 (d, J=8.0 Hz, 1H), 6.37 (s, 1H), 4.21–4.11 (m, 2H), 2.44 (s, 3H), 1.28 (t, J=7.0 Hz, 3H) ppm; ^{13}C NMR (100 MHz, $CDCl_3$): δ 166.6, 163.5, 155.2, 140.0, 137.9, 134.3, 129.0 (×2), 128.7 (×2), 126.8, 124.2, 123.9, 122.4, 111.7, 102.9, 60.3, 57.3, 23.9, 14.5 ppm; IR (KBr): ν_{max} 3418, 2978, 1698, 1671, 1585, 1503, 1410, 1370, 1328, 1271, 1239, 1202, 1089, 1076, 1013, 978, 835, 742 cm^{-1}; LRMS (ESI+): *m/z* calcd for $C_{20}H_{18}ClN_2O_2S$ $[M+H]^+$ 385.1; found 385.1.

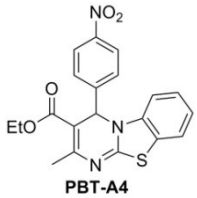

PBT-A4

Ethyl 2-methyl-4-(4-nitrophenyl)-4*H*-pyrimido[2,1-*b*][1,3]benzothiazole-3-carboxylate (PBT-A4). The reaction of 4-nitrobenzaldehyde (181 mg, 1.2 mmol), ethyl acetoacetate (195 mg, 1.5 mmol), 2-aminobenzothiazole (150 mg, 1.0 mmol), and $Hf(OTf)_4$ (8 mg, 0.01 mmol) followed by flash column chromatography (PE/EA=10:1) afforded **PBT-A4** (288 mg, 73%) as a yellow solid; mp 171–172 °C. Single crystal was cultured by recrystallization from CH_2Cl_2/hexane. ^{1}H NMR (400 MHz, $CDCl_3$): δ 8.13 (d, J=8.6 Hz, 2H), 7.61 (d, J=8.6 Hz, 2H), 7.49 (d, J=8.1 Hz, 1H), 7.26 (dd, J_1=J_2=6.4 Hz, 1H), 7.18 (dd, J_1=J_2=6.4 Hz, 1H), 7.04 (d, J=8.1 Hz, 1H), 6.53 (s, 1H), 4.24–4.16 (m, 2H), 2.46 (s, 3H), 1.31 (t, J=6.5 Hz, 3H) ppm; ^{13}C NMR (100 MHz, $CDCl_3$): δ 166.5, 163.7, 156.0, 148.1, 147.9, 137.7, 128.2 (×2), 127.0, 124.6, 124.2 (×2), 124.0, 122.6, 111.5, 102.2, 60.6, 57.2, 24.1, 14.5 ppm; IR (KBr): ν_{max} 3434, 2979, 1700, 1670, 1584, 1500, 1348, 1273, 1242, 1202, 1076, 979, 820, 746 cm^{-1}; LRMS (ESI+): *m/z* calcd for $C_{20}H_{18}N_3O_4S$ $[M+H]^+$ 396.1; found 396.1.

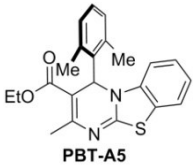

PBT-A5

Ethyl 2-methyl-4-(2,6-dimethylphenyl)-4*H*-pyrimido[2,1-*b*][1,3]benzothiazole-3-carboxylate (PBT-A5). The reaction of 2,6-dimethylbenzaldehyde (161 mg, 1.2 mmol), ethyl acetoacetate (195 mg, 1.5 mmol), 2-aminobenzothiazole (150 mg, 1.0 mmol), and $Hf(OTf)_4$ (8 mg, 0.01 mmol) followed by flash column chromatography (PE/EA=10:1) afforded **PBT-A5** (208 mg, 55%) as a yellow solid; mp 169–170 °C. Single crystal was cultured by recrystallization from CH_2Cl_2/hexane. ^{1}H NMR (400 MHz, $CDCl_3$): δ 7.38 (d, J=7.4 Hz, 1H), 7.08–7.03 (m, 4H), 6.91 (s, 2H), 6.71 (d, J=7.3 Hz, 1H), 4.06 (q, J=7.1 Hz, 2H), 2.85 (s, 3H), 2.29 (s, 3H), 2.22 (s, 3H), 1.13 (t, J=7.1 Hz, 3H) ppm; ^{13}C NMR (100 MHz, $CDCl_3$): δ 167.4, 162.9, 151.2, 139.0, 138.9, 137.3, 135.2, 131.4, 129.1, 128.2, 126.7, 123.7, 122.9, 122.0, 112.0, 102.0, 60.1, 55.9, 23.5, 21.3, 19.4, 14.4 ppm; IR (KBr): ν_{max} 3670, 2978, 1682, 1583, 1519, 1466, 1363, 1326, 1268, 1239, 1198, 1076, 978, 821, 744 cm^{-1}; HRMS (ESI+): *m/z* calcd for $C_{22}H_{23}N_2O_2S$ $[M+H]^+$ 379.1475; found 379.1476.

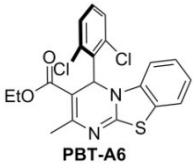

PBT-A6

Ethyl 2-methyl-4-(2,6-dichlorophenyl)-4*H*-pyrimido[2,1-*b*][1,3]benzothiazole-3-carboxylate (PBT-A6). The reaction of 2,6-dichlorobenzaldehyde (210 mg, 1.2 mmol), ethyl acetoacetate (195 mg, 1.5 mmol), 2-aminobenzothiazole (150 mg, 1.0 mmol), and $Hf(OTf)_4$ (8 mg, 0.01 mmol) followed by flash column chromatography (PE/EA=8:1) afforded **PBT-A6** (188 mg, 45%) as a yellow solid; mp 247–248 °C. Single crystal was cultured by recrystallization from CH_2Cl_2/hexane. ^{1}H NMR (400 MHz, $CDCl_3$): δ 7.40 (d, J=7.9 Hz, 1H), 7.35 (d, J=7.9 Hz, 1H), 7.27–7.25 (m, 3H), 7.21–7.18 (m, 1H), 7.14–7.09 (m, 2H), 4.15–4.08 (m, 2H), 2.40 (s, 3H), 1.16 (t,

J=7.1 Hz, 3H) ppm; ^{13}C NMR (100 MHz, $CDCl_3$): δ 166.5, 163.7, 156.3, 138.7, 137.1, 136.6, 133.7, 131.2, 129.8, 128.6, 126.8, 124.0, 123.2, 122.1, 111.9, 99.1, 59.9, 55.8, 24.1, 14.5 ppm; IR (KBr): ν_{max} 3436, 3073, 2927, 1682, 1576, 1500, 1432, 1371, 1334, 1274, 1248, 1202, 1173, 1080, 1009, 981, 834, 790, 750 cm^{-1}; LRMS (ESI+): *m/z* calcd for $C_{20}H_{17}Cl_2N_2O_2S$ $[M+H]^+$ 419.0; found 419.0.

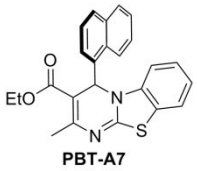

PBT-A7

Ethyl 2-methyl-4-(naphthyl)-4*H*-pyrimido[2,1-*b*][1,3]benzothiazole-3-carboxylate (PBT-A7). The reaction of 1-naphthaldehyde (187 mg, 1.2 mmol), ethyl acetoacetate (195 mg, 1.5 mmol), 2-aminobenzothiazole (150 mg, 1.0 mmol), and $Hf(OTf)_4$ (8 mg, 0.01 mmol) followed by flash column chromatography (PE/EA=10:1) afforded **PBT-A7** (336 mg, 84%) as a yellow solid; mp 168–169 °C. Single crystal was cultured by recrystallization from CH_2Cl_2/hexane. ^{1}H NMR (400 MHz, $CDCl_3$): δ 8.64 (d, *J*=8.0 Hz, 1H), 7.82–7.79 (m, 2H), 7.73–7.66 (m, 2H), 7.50 (dd, J_1=J_2= 7.5 Hz, 1H), 7.40–7.35 (m, 2H), 7.19 (s, 1H), 7.04–6.99 (m, 3H), 4.05–3.97 (m, 2H), 2.50 (s, 3H), 1.07 (t, *J*=7.1 Hz, 3H) ppm; ^{13}C NMR (100 MHz, $CDCl_3$): δ 166.8, 163.3, 154.2, 139.2, 138.7, 133.4, 130.5, 129.4, 129.2, 127.7, 127.0, 126.7, 126.0, 125.8, 123.9, 123.6, 123.4, 122.1, 111.9, 104.1, 60.1, 54.2, 23.9, 14.4 ppm; IR (KBr): ν_{max} 3388, 2975, 1698, 1586, 1504, 1369, 1327, 1269, 1241, 1199, 1168, 1076, 977, 778, 742 cm^{-1}; HRMS (ESI+): *m/z* calcd for $C_{24}H_{21}N_2O_2S$ $[M+H]^+$ 401.1318; found401.1321.

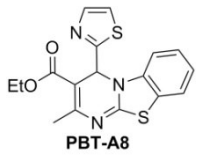

PBT-A8

Ethyl 2-methyl-4-(thiazolyl)-4*H*-pyrimido[2,1-*b*][1,3]benzothiazole-3-carboxylate (PBT-A8). The reaction of 1,3-thiazole-2-carbaldehyde (136 mg, 1.2 mmol), ethyl acetoacetate (195 mg, 1.5 mmol), 2-aminobenzothiazole (150 mg, 1.0 mmol), and $Hf(OTf)_4$ (8 mg, 0.01 mmol) followed by flash column chromatography (PE/EA=10:1) afforded **PBT-A8** (221 mg, 62%) as a yellow solid; mp 151–152 °C. Single crystal was cultured by recrystallization from CH_2Cl_2/hexane. ^{1}H NMR (400 MHz, $CDCl_3$): δ 7.63 (d, *J*=3.2 Hz, 1H), 7.55 (d, *J*=8.2 Hz, 1H), 7.46 (d, *J*=8.2 Hz, 1H), 7.34 (dd, J_1=J_2=7.6 Hz, 1H), 7.23 (d, *J*=3.2 Hz, 1H), 7.19 (dd, J_1=J_2=7.6 Hz, 1H), 6.85 (s, 1H), 4.25–4.16 (m, 2H), 2.51 (s, 3H), 1.25 (t, *J* =7.1 Hz, 3H) ppm; ^{13}C NMR (100 MHz, $CDCl_3$): δ 169.5, 166.2, 163.5, 157.5, 142.8, 138.0, 126.8, 124.4, 123.8, 122.3, 120.7, 112.6, 100.7, 60.4, 54.4, 23.8, 14.5 ppm; IR (KBr): ν_{max} 3407, 3104, 2975, 2894, 1666, 1584, 1505, 1491, 1372, 1326, 1247, 1201, 1101, 979, 793, 750 cm^{-1}; HRMS (ESI+): *m/z* calcd for $C_{17}H_{16}N_3O_2S_2$ $[M+H]^+$ 358.0678; found 358.0679.

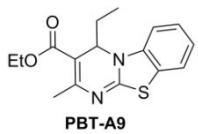

PBT-A9

Ethyl 2-methyl-4-(ethyl)-4*H*-pyrimido[2,1-*b*][1,3]benzothiazole-3-carboxylate (PBT-A9). The reaction of propionaldehyde (70 mg, 1.2 mmol), ethyl acetoacetate (195 mg, 1.5 mmol), 2-aminobenzothiazole (150 mg, 1.0 mmol), and $Hf(OTf)_4$ (8 mg, 0.01 mmol) in a sealed tube followed by flash column chromatography (PE/EA=12:1) afforded **PBT-A9** (145 mg, 48%) as a yellow solid; mp 97–98 °C. ^{1}H NMR (400 MHz, $CDCl_3$): δ 7.48 (d, J=7.6 Hz, 1H), 7.35 (dd, J_1=J_2=7.6 Hz, 1H), 7.21–7.18 (m, 2H), 5.62 (t, J=3.8 Hz, 1H), 4.27–4.21 (m, 2H), 2.42 (s, 3H), 1.91–1.87 (m, 1H), 1.66–1.62 (m, 1H), 1.34 (t, J=7.1 Hz, 3H), 0.80 (t, J=7.1 Hz, 3H) ppm; ^{13}C NMR (100 MHz, $CDCl_3$): δ 167.1, 164.4, 157.4, 138.3, 126.8, 124.3, 123.9, 122.5, 111.2, 100.0, 60.1, 54.3, 26.8, 23.7, 14.7, 8.0 ppm; IR (KBr): ν_{max} 3379, 2969, 1698, 1672, 1586, 1505, 1459, 1362, 1331, 1270, 1237, 1204, 1099, 1076, 1064, 969, 747 cm^{-1}; HRMS (ESI+): *m/z* calcd for $C_{16}H_{19}N_2O_2S$ $[M+H]^+$ 303.1162; found 303.1166.

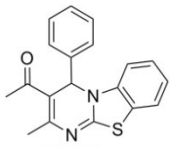

PBT-B1

2-Methyl-4-(phenyl)-4*H*-pyrimido[2,1-*b*][1,3]benzothiazole-3-ethanone (PBT-B1). The reaction of benzaldehyde (1.27 g, 12.0 mmol), 2,4-pentanedione (1.5 g, 15.0 mmol), 2-amino-benzothiazole (1.5 g, 10.0 mmol), and $Hf(OTf)_4$ (80 mg, 0.1 mmol) followed by flash column chromatography (PE/EA=8:1) afforded **PBT-B1** (2.53 g, 79%) as a yellow solid; mp 199–200 °C. Single crystal was cultured by recrystallization from CH_2Cl_2/hexane. ^{1}H NMR (400 MHz, $CDCl_3$): δ 7.45–7.39 (m, 3H), 7.24–7.20 (m, 3H), 7.17–7.11 (m, 3H), 6.55 (s, 1H), 2.42 (s, 3H), 2.38 (s, 3H) ppm; ^{13}C NMR (100 MHz, $CDCl_3$): δ 195.5, 163.8, 154.5, 141.4, 138.3, 128.8 (×2), 128.3, 127.2 (×2), 127.0, 124.2, 124.1, 122.3, 114.4, 112.2, 57.1, 32.0, 25.3 ppm; IR (KBr): ν_{max} 3399, 3034, 2921, 1610, 1561, 1477, 1355, 1318, 1264, 1244, 1200, 1116, 1025, 1012, 953, 931, 735 cm^{-1}; LRMS (ESI+): *m/z* calcd for $C_{19}H_{17}N_2OS$ $[M+H]^+$ 321.1; found 321.1.

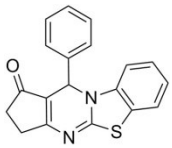

PBT-B2

11-Phenyl-3,11-dihydrobenzo[4,5]thiazolo[3,2-*a*]cyclopenta[*d*]pyrimidin-1(2*H*)-one (PBT-B2). The reaction of benzaldehyde (254 mg, 2.4 mmol), 1,3-cyclopentanedione (294 mg, 3.0 mmol), 2-aminobenzothiazole (300 mg, 2.0 mmol), and $Hf(OTf)_4$ (15 mg, 0.2 mmol) followed by flash column chromatography (DCM/EA=8:1) afforded **PBT-B2** (382 mg, 60%) as a yellow solid; mp 255–256 °C. Single crystal was cultured by recrystallization from CH_2Cl_2/hexane. ^{1}H NMR (400 MHz, $CDCl_3$): δ 7.52 (d, J=7.5 Hz, 1H), 7.35 (d, J=7.5 Hz, 2H), 7.28 (dd, J_1=J_2=7.5 Hz, 2H), 7.24–7.17 (m, 3H), 6.95 (d, J=7.5 Hz, 1H), 6.41 (s, 1H), 2.71–2.66 (m, 2H), 2.46–2.42 (m, 2H) ppm; ^{13}C NMR (100 MHz, $CDCl_3$): δ 202.0, 174.0, 168.3, 139.6, 138.4, 129.1 (×2), 128.6, 127.2, 126.2 (×2), 124.6, 123.8, 122.5, 115.3, 112.8, 58.3, 35.0, 28.5 ppm; IR (KBr): ν_{max} 3428, 2928, 1660, 1591, 1471, 1448, 1391, 1354, 1266, 1199, 1112, 1084, 1045, 936, 836, 801, 744 cm^{-1}; HRMS (ESI+): *m/z* calcd for $C_{19}H_{15}N_2OS$ $[M+H]^+$ 319.0900; found 319.0903.

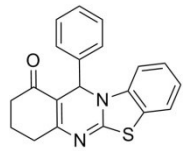

PBT-B3

12-Phenyl-2,3,4,12-tetrahydro-1*H*-benzo[4,5]thiazolo[2,3-*b*]quinazolin-1-one (PBT-B3). The reaction of benzaldehyde (254 mg, 2.4 mmol), 1,3-cyclohexanedione (336 mg, 3.0 mmol), 2-aminobenzothiazole (300 mg, 2.0 mmol), and $Hf(OTf)_4$ (15 mg, 0.2 mmol) followed by flash column chromatography (DCM/EA=10:1) afforded **PBT-B3** (405 mg, 61%) as a yellow solid; mp 254–255 °C. Single crystal was cultured by recrystallization from CH_2Cl_2/hexane. ^{1}H NMR (400 MHz, $CDCl_3$): δ 7.47 (d, J=7.8 Hz, 1H), 7.40 (d, J=7.8 Hz, 2H), 7.26–7.22 (m, 3H), 7.19–7.09 (m, 3H), 6.53 (s, 1H), 2.67–2.56 (m, 2H), 2.39–2.34 (m, 2H), 2.01–1.89 (m, 2H) ppm; ^{13}C NMR (100 MHz, $CDCl_3$): δ 195.8, 165.6, 160.5, 141.1, 138.5, 128.8 (×2), 128.3, 127.1 (×2), 127.0, 124.4, 123.8, 122.3, 112.5, 111.7, 56.1, 37.4, 31.7, 21.5 ppm; IR (KBr): ν_{max} 3434, 1621, 1579, 1486, 1376, 1328, 1270, 1215, 1181, 1114, 1046, 998, 885, 827, 779, 743 cm^{-1}; LRMS (ESI+): *m/z* calcd for $C_{20}H_{17}N_2OS$ $[M+H]^+$ 333.4; found 333.4.

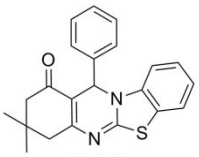

PBT-B4

3,3-Dimethyl-12-phenyl-2,3,4,12-tetrahydro-1*H*-benzo[4,5]thiazolo[2,3-*b*]quinazolin-1(2*H*)-one (PBT-B4). The reaction of benzaldehyde (127 mg, 1.2 mmol), 5,5-dimethyl-1,3-cyclohexanedione (140 mg, 1.0 mmol), 2-aminobenzothiazole (150 mg, 1.0 mmol), and $Hf(OTf)_4$ (8 mg, 0.01 mmol) followed by flash column chromatography (DCM/EA=10:1) afforded **PBT-B4** (299 mg, 83%) as a yellow solid; mp 238–239 °C. Single crystal was cultured by recrystallization from CH_2Cl_2/hexane. ^{1}H NMR (400 MHz, $CDCl_3$): δ 7.48 (d, J=7.6 Hz, 1H), 7.43 (d, J=7.2 Hz, 2H), 7.29–7.21 (m, 3H), 7.20–7.11 (m, 3H), 6.51 (s, 1H), 2.49 (s, 2H), 2.23 (q, J=16.4 Hz, 2H), 1.08 (s, 3H), 0.93 (s, 3H) ppm; ^{13}C NMR (100 MHz, $CDCl_3$): δ 195.7, 165.8, 158.7, 140.8, 138.5, 128.8 (×2), 128.3, 127.1 (×3), 124.4, 123.9, 122.3, 112.5, 110.6, 56.3, 51.1, 45.6, 32.8, 29.4, 27.5 ppm; IR (KBr): ν_{max} 3028, 250, 2869, 1625, 1584, 1482, 1377, 1356, 1325, 1276, 1237, 1204, 1167, 1144, 1116, 1507, 1027, 832, 801, 744 cm^{-1}; LRMS (ESI+): *m/z* calcd for $C_{22}H_{21}N_2OS$ $[M+H]^+$ 361.1; found 361.1.

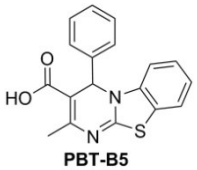

PBT-B5

2-Methyl-4-(phenyl)-4*H*-pyrimido[2,1-*b*][1,3]benzothiazole-3-carboxylic acid (PBT-B5). To a solution of **PBT-1** (700 mg, 2.0 mmol) in THF/EtOH/H_2O (20 mL, 2:1:1) was added $LiOH{\cdot}H_2O$ (420 mg, 10.0 mmol). The reaction was stirred in a sealed tube at 80 °C for 6 h. Flash column chromatography (DCM/MeOH=30:1) afforded **PBT-B5** (535 mg, 83%) as a yellow solid; mp 166–167 °C. Single crystal was cultured by recrystallization from CH_2Cl_2/hexane. ^{1}H NMR (400 MHz, DMSO-d_6): δ 12.18 (s, 1H), 7.71 (d, J=7.8 Hz, 1H), 7.43–7.40 (m, 3H), 7.30–7.26 (m, 3H),

7.21–7.14 (m, 2H), 6.45 (s, 1H), 2.32 (s, 3H) ppm; ^{13}C NMR (100 MHz, DMSO-d_6): δ 167.3, 162.3, 153.3, 141.5, 137.6, 128.5 (×2), 128.1, 126.9 (×3), 126.7, 123.8, 122.7, 112.1, 103.5, 56.6, 23.0 ppm; IR (KBr): ν_{max}3387, 1659, 1580, 1481, 1399, 1360, 1320, 1252, 1202, 1092, 1017, 976, 813, 737 cm^{-1}; LRMS (ESI+): *m/z* calcd for $C_{18}H_{15}N_2O_2S$ $[M+H]^+$ 323.1; found 323.1.

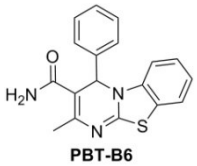

PBT-B6

2-Methyl-4-(phenyl)-4*H*-pyrimido[2,1-*b*][1,3]benzothiazole-3-amide (PBT-B6). To a solution of **PBT-B5** (322 mg, 1.0 mmol) in DCM was added EDC·HCl (211 mg, 1.1 mmol) and HOBt (162 mg, 1.2 mmol). After 30 min, conc. $NH_3·H_2O$ (20 eq) in THF (1 mL) was added. The reaction was stirred for 1 h and concentrated *in vacuo*. Flash column chromatography (DCM/MeOH=30:1) afforded **PBT-B6** (258 mg, 80%) as a yellow solid; mp 146–147 °C. Single crystal was cultured by recrystallization from CH_2Cl_2/hexane. ^{1}H NMR (400 MHz, MeOH-d_4): δ 7.56 (d, *J*=8.0 Hz, 1H), 7.34–7.27 (m, 4H), 7.23 (dd, J_1=J_2=7.5 Hz, 2H), 7.15 (dd, J_1=J_2=7.5 Hz, 1H), 7.07 (d, *J*=8.0 Hz, 1H), 6.49 (s, 1H), 2.15 (s, 3H) ppm; ^{13}C NMR (100 MHz, MeOH-d_4): δ 172.8, 163.6, 143.2, 141.7, 139.3, 130.0 (×2), 129.6, 127.8, 127.6 (×2), 125.2, 124.2, 123.4, 113.2, 110.5, 59.7, 21.5 ppm; IR (KBr): ν_{max} 3424, 2960, 1654, 1542, 1469, 1395, 1358, 1304, 1270, 1205, 1125, 1101, 1020, 983, 943, 925, 852, 828, 742 cm^{-1}; HRMS (ESI+): *m/z* calcd for $C_{18}H_{16}N_3OS$ $[M+H]^+$ 322.1009; found 322.1009.

PBT-C1

Ethyl 4-phenyl-2-(trifluoromethyl)-4*H*-pyrimido[2,1-*b*][1,3]benzothiazole-3-carboxylate (PBT-C1). The reaction of benzaldehyde (127 mg, 1.2 mmol), ethyl 4,4,4-trifluoroacetoacetate (276 mg, 1.5 mmol), 2-aminobenzothiazole (150 mg, 1.0 mmol), and $Hf(OTf)_4$ (8 mg, 0.01 mmol) followed by flash column chromatography afforded (PE/EA=15:1) **PBT-C1** (267 mg, 66%) as a yellow solid; mp 164–165 °C. Single crystal was cultured by recrystallization from CH_2Cl_2/hexane. ^{1}H NMR (400 MHz, $CDCl_3$): δ 7.48 (d, *J*=7.6 Hz, 1H), 7.40–7.38 (m, 2H), 7.32–7.22 (m, 4H), 7.17 (dd, J_1=J_2=7.6 Hz, 1H), 7.03 (d, *J*=8.0 Hz, 1H), 6.45 (s, 1H), 4.21–4.12 (m, 2H), 1.26–1.19 (m, 3H) ppm; ^{13}C NMR (100 MHz, $CDCl_3$): δ 165.2, 163.7, 139.4, 139.2, 138.8, 137.4, 129.4, 129.3, 127.0 (×2), 124.6, 124.2, 122.4, 121.3 (q, *J*=273 Hz), 112.2 (×2), 108.2, 61.6, 59.0, 13.9 ppm; ^{19}F NMR (470 MHz, $CDCl_3$): δ -65.24 ppm; IR (KBr): ν_{max} 3427, 2994, 1697, 1584, 1533, 1355, 1296, 1273, 1256, 1225, 1195, 1148, 1094, 1022, 922, 906, 743 cm^{-1}; LRMS (ESI+): *m/z* calcd for $C_{20}H_{16}F_3N_2O_2S$ $[M+H]^+$ 405.1; found 405.1.

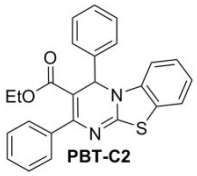

PBT-C2

Ethyl 2,4-diphenyl-4*H*-pyrimido[2,1-*b*][1,3]benzothiazole-3-carboxylate (PBT-C2). The reaction of benzaldehyde (127 mg, 1.2 mmol), ethyl benzoylacetate (288 mg, 1.5 mmol), 2-aminobenzothiazole (150 mg, 1.0 mmol), and $Hf(OTf)_4$ (8 mg, 0.01 mmol) followed by flash

column chromatography (PE/EA=15:1) afforded **PBT-C2** (239 mg, 58%) as a yellow solid; mp 150–151 °C. Single crystal was cultured by recrystallization from CH_2Cl_2/hexane. ^{1}H NMR (400 MHz, $CDCl_3$): δ 7.54–7.52 (m, 2H), 7.45–7.43 (m, 1H), 7.39–7.37 (m, 2H), 7.34–7.27 (m, 5H), 7.24–7.20 (m, 2H), 7.15–7.11 (m, 2H), 6.52 (s, 1H), 3.90–3.83 (m, 2H), 1.25 (t, *J*=7.2 Hz, 3H) ppm; ^{13}C NMR (100 MHz, $CDCl_3$): δ 166.9, 163.6, 154.9, 141.5, 141.0, 138.2, 129.0 (×2), 128.6, 128.4, 128.3 (×2), 127.8 (×2), 127.3 (×2), 126.8, 124.3, 124.2, 122.3, 112.0, 103.4, 60.1, 58.4, 13.7 ppm; IR (KBr): ν_{max} 3347, 3098, 3043, 2978, 1673, 1506, 1482, 1369, 1334, 1254, 1216, 1092, 1031, 921, 910, 744 cm^{-1}; LRMS (ESI+): *m/z* calcd for $C_{25}H_{21}N_2O_2S$ $[M+H]^+$ 413.1; found 413.1.

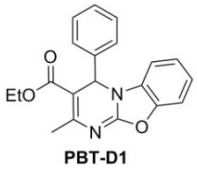

PBT-D1

Ethyl 2-methyl-4-(phenyl)-4*H*-pyrimido[2,1-*b*][1,3]benzoxazole-3-carboxylate (PBT-D1). The reaction of benzaldehyde (254 mg, 2.4 mmol), ethyl acetoacetate (390 mg, 3.0 mmol), 2-aminobenzoxazole (268 mg, 2.0 mmol), and $Hf(OTf)_4$ (15 mg, 0.02 mmol) followed by flash column chromatography (PE/EA=12:1) afforded **PBT-D1** (170 mg, 51%) as a white solid; mp 156–157 °C. Single crystal was cultured by recrystallization from CH_2Cl_2/hexane. ^{1}H NMR (400 MHz, $CDCl_3$): δ 7.44 (d, *J*=7.2 Hz, 2H), 7.31–6.21 (m, 4H), 7.10–7.07 (m, 2H), 6.91–6.88 (m, 1H), 6.34 (s, 1H), 4.15–4.03 (m, 2H), 2.52 (s, 3H), 1.22 (t, *J*=7.1 Hz, 3H) ppm; ^{13}C NMR (100 MHz, $CDCl_3$): δ 166.3, 157.3, 156.5, 144.8, 140.9, 129.7, 128.8 (×2), 127.8 (×2), 124.7, 123.6 (×2), 110.5, 109.9, 102.9, 60.1, 50.9, 24.2, 14.4 ppm; IR (KBr): ν_{max} 3065, 3037, 2976, 1691, 1644, 1621, 1537, 1479, 1406, 1374, 1335, 1246, 1191, 1143, 1099, 1075, 1006, 980, 832, 798, 743 cm^{-1}; HRMS (ESI+): *m/z* calcd for $C_{20}H_{19}N_2O_3$ $[M+H]^+$ 335.1390; found 335.1395.

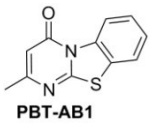

PBT-AB1

2-Methyl-4*H*-pyrimido[2,1-*b*][1,3]benzothiazol-4-one (PBT-AB1). To a mixture of ethyl acetoacetate (390 mg, 3.0 mmol) and 2-aminobenzothiazole (300 mg, 2.0 mmol) was added $Hf(OTf)_4$ (77 mg, 0.1 mmol). The reaction was stirred at 120 °C for 12 h. Upon cooling, the solid precipitate was collected by filtration. Recrystallization from ethanol afforded **PBT-AB1** (346 mg, 80%) as a white crystal; mp 205–206 °C. ^{1}H NMR (400 MHz, $CDCl_3$): δ 9.03–9.01 (m, 1H), 7.65–7.62 (m, 1H), 7.50–7.42 (m, 2H), 6.22 (s, 1H), 2.36 (s, 3H) ppm; ^{13}C NMR (100 MHz, $CDCl_3$): δ 163.0, 161.5, 161.2, 136.2, 127.1, 127.0, 124.2., 121.8, 120.1, 107.3, 23.8 ppm; IR (KBr): ν_{max} 3379, 1675, 1575, 1530, 1460, 1439, 1394, 1364, 1240, 1162, 1038, 980, 823, 764, 738 cm^{-1}; LRMS (ESI+): *m/z* calcd for $C_{11}H_9N_2OS$ $[M+H]^+$ 217.0; found 217.0.

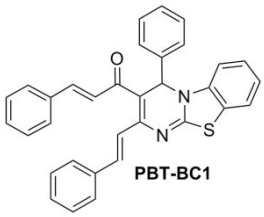

PBT-BC1

(*E*)-3-Phenyl-1-(4-phenyl-2-((*E*)-styryl)-4*H*-pyrimido[2,1-*b*][1,3]benzothiazole-3-yl)prop-2-en-1-one (PBT-BC1). The reaction of **PBT-B1** (320 mg, 1.0 mmol) and benzaldehyde (424 mg,

4.0 mmol) followed by flash column chromatography (PE/EA=15:1) afforded **PBT-BC1** (372 mg, 75%) as an orange solid; mp 187–188 °C. ^{1}H NMR (400 MHz, $CDCl_3$): δ 7.75 (d, J=15.4 Hz, 1H), 7.32–7.23 (m, 9H), 7.19–7.12 (m, 10H), 7.53–7.42 (m, 3H), 6.58 (s, 1H) ppm; ^{13}C NMR (100 MHz, $CDCl_3$): δ 189.9, 163.6, 149.4, 141.3, 141.1, 138.4, 137.0, 136.7, 135.4. 130.2, 129.0 (×5), 128.9 (×2), 128.5, 128.2 (×2), 128.1, 127.7 (×2), 127.1 (×2), 126.9, 125.5, 124.1, 122.4, 114.7, 112.0 (×2), 58.1 ppm; IR (KBr): ν_{max} 3435, 3058, 2970, 1620, 1572, 1481, 1446, 1346, 1275, 1196, 1082, 1048, 990, 970, 743 cm^{-1}; HRMS (ESI+): *m/z* calcd for $C_{33}H_{25}N_2OS$ $[M+H]^+$ 497.1682; found 497.1683.

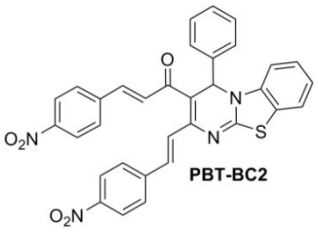

PBT-BC2

(*E*)-3-(4-Nitrophenyl)-1-(2-((*E*)-4-nitrophenyl)-4-phenyl-4*H*-pyrimido[2,1-*b*][1,3]benzothiazol-3-yl)prop-2-en-1-one (PBT-BC2). The reaction of **PBT-B1** (320 mg, 1.0 mmol) and 4-nitrobenzaldehyde (604 mg, 4.0 mmol) followed by flash column chromatography (PE/EA=15:1) afforded **PBT-BC2** (357 mg, 61%) as a red solid; ^{1}H NMR (400 MHz, $CDCl_3$): δ 8.20–8.14 (m, 4H), 7.82 (d, J=15.4 Hz, 1H), 7.61–7.46 (m, 10H), 7.30–7.18 (m, 6H), 6.58 (s, 1H) ppm; ^{13}C NMR (100 MHz, $CDCl_3$): δ 188.9, 164.2, 148.9, 148.7, 147.9, 142.8, 141.3, 140.7, 138.8, 138.2, 134.8, 131.1, 129.2 (×2), 128.9 (×2), 128.6, 128.0 (×2), 127.2, 127.0 (×2), 124.6, 124.5 (×2), 124.4 (×2), 124.2, 122.6, 115.5, 112.2, 58.3, 29.9 ppm; IR (KBr): ν_{max} 3439, 2956, 1638, 1594, 1514, 1410, 1339, 1275, 1197, 1108, 990, 974, 842, 744 cm^{-1}; HRMS (ESI+): *m/z* calcd for $C_{33}H_{23}N_4O_5S$ $[M+H]^+$ 587.1384; found 587.1385.

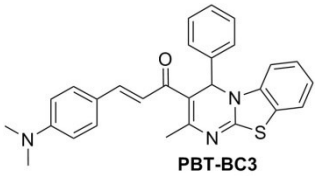

PBT-BC3

(*E*)-3-(4-(Dimethylamino)phenyl)-1-(2-methyl-4-phenyl-4*H*-pyrimido[2,1-*b*][1,3]benzothiazol-3-yl)prop-2-en-1-one (PBT-BC3). The reaction of **PBT-B1** (320 mg, 1.0 mmol) and 4-dimethylaminobenzaldehyde (596 mg, 4.0 mmol) followed by flash column chromatography (PE/EA = 8:1) afforded **PBT-BC3** (248 mg, 55%) as an orange solid; mp 204–205 °C. Two single crystal polymorphs (orange-colored and red-colored) were cultured by recrystallization from CH_2Cl_2/ether and methanol, respectively. ^{1}H NMR (400 MHz, $CDCl_3$): δ 7.43–7.36 (m, 6H), 7.25–7.03 (m, 6H), 6.81 (d, J=15.6 Hz, 1H), 6.64–6.60 (m, 3H), 2.99 (s, 6H), 2.33 (s, 3H) ppm; ^{13}C NMR (100 MHz, $CDCl_3$): δ 191.9, 162.6, 151.9, 148.7, 143.2, 141.3, 138.5, 130.1 (×2), 128.9 (×2), 128.3, 126.8 (×2), 126.7, 123.8, 123.7, 123.0, 122.7, 122.2, 114.9, 112.0, 111.9 (×2), 58.3, 40.3 (×2), 24.2 ppm; IR (KBr): ν_{max} 3440, 2911, 1628, 1605, 1567, 1521, 1432, 1340, 1269, 1182, 1167, 1051, 1026, 973, 946, 816, 743 cm^{-1}; HRMS (ESI+): *m/z* calcd for $C_{28}H_{26}N_3OS$ $[M+H]^+$ 452.1791; found 452.1794.

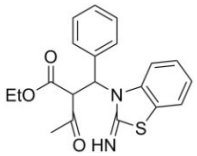

Ethyl 2-((2-iminobenzo[d]thiazol-3(2*H*)-yl)(phenyl)methyl)-3-oxobutanoate (key intermediate for PBT-1). The reaction of benzaldehyde (127 mg, 1.2 mmol), ethyl acetoacetate (195 mg, 1.5 mmol), and 2-aminobenzothiazole (150 mg, 1.0 mmol) was added $Hf(OTf)_4$ (8 mg, 0.01 mmol) for ONLY 45 min followed by flash column chromatography (PE/EA=10:1) afforded the **key intermediate** (155 mg, 42%) as colorless oil. ^{1}H NMR (400 MHz, $CDCl_3$): δ 7.55–7.52 (m, 2H), 7.39 (d, J=12.5 Hz, 2H), 7.33–7.23 (m, 5H), 7.08–7.04 (m, 1H), 5.81, 5.66 (s, 1H), 4.14–4.05 (m, 3H), 2.30, 2.19 (s, 3H), 1.14–1.09 (m, 3H) ppm; ^{13}C NMR (100 MHz, $CDCl_3$): δ 203.4 (200.9), 168.8 (167.1), 166.5 (166.3), 152.2, 138.9 (138.8), 130.9, 128.9, 128.2 (128.1), 127.0, 126.6, 126.0, 122.0 (121.9), 121.0, 119.4 (119.3), 64.7 (63.7), 62.2 (62.0), 58.5 (57.4), 31.0, 29.4, 14.0 ppm; IR (KBr): ν_{max} 3435, 2982, 1716, 1600, 1538, 1494, 1445, 1358, 1249, 1209, 1155, 1018, 754 cm^{-1}; HRMS (ESI+): *m/z* calcd for $C_{20}H_{21}N_2O_3S$ $[M+H]^+$ 369.1267; found 369.1269.

3. Synthetic and mechanistic investigations on $Hf(OTf)_4$-catalyzed 3CR

3.1 Catalytic effect comparison

Table S1 Comparison of $Hf(OTf)_4$ with other reported catalysts and reaction optimization[a]

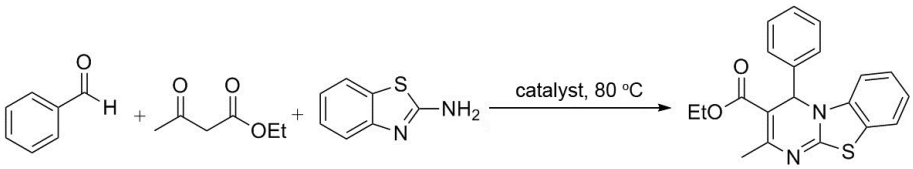

catalyst	mol%	solvent	reaction time (h)	isolated yield
no	0	no	24	31
L-proline[1]	10	no	24	33 (87, 4 h)[b]
camphor sulfonic acid[2]	10	EtOH	24	35 (90, 8 h)[b]
NH_2SO_3H[3]	10	EtOH	24	47 (86, 1 h)[b]
CH_3COOH[1]	10	no	24	49 (67, 18 h)[b]
$AlCl_3$[4]	10	no	16	87 (79, 1 h)[b]
$Hf(OTf)_4$	10	no	3	91
$Hf(OTf)_4$	1	no	6	90

[a]Reactions were performed with benzaldehyde (1.2 mmol), ethyl acetoacetate (1.5 mmol), and 2-aminobenzothiazole (1.0 mmol). [b]Reported yield and reaction time in references.

References:

1. P. K. Sahu, P. K. Sahu, P. Samadhiya, P. L. Sahu, D. D. Agarwal, *Med. Chem. Res.*, 2016, **21**, 1551–1563.
2. S. Seenan and S. K. Iyer, *J. Org. Chem.*, 2020, **85**, 1871–1881.
3. R. M. Kumbhare and C. Nagragu *Lett. Drug Des. Disco.* 2011, **8**, 633–639.
4. P. K. Sahu, P. K. Sahu, J. Lal, D. Thavaselvam, D. D. Agarwal, *Med. Chem. Res.*, 2012, **21**, 3826–3834.

3.2 Identification of reaction pathway

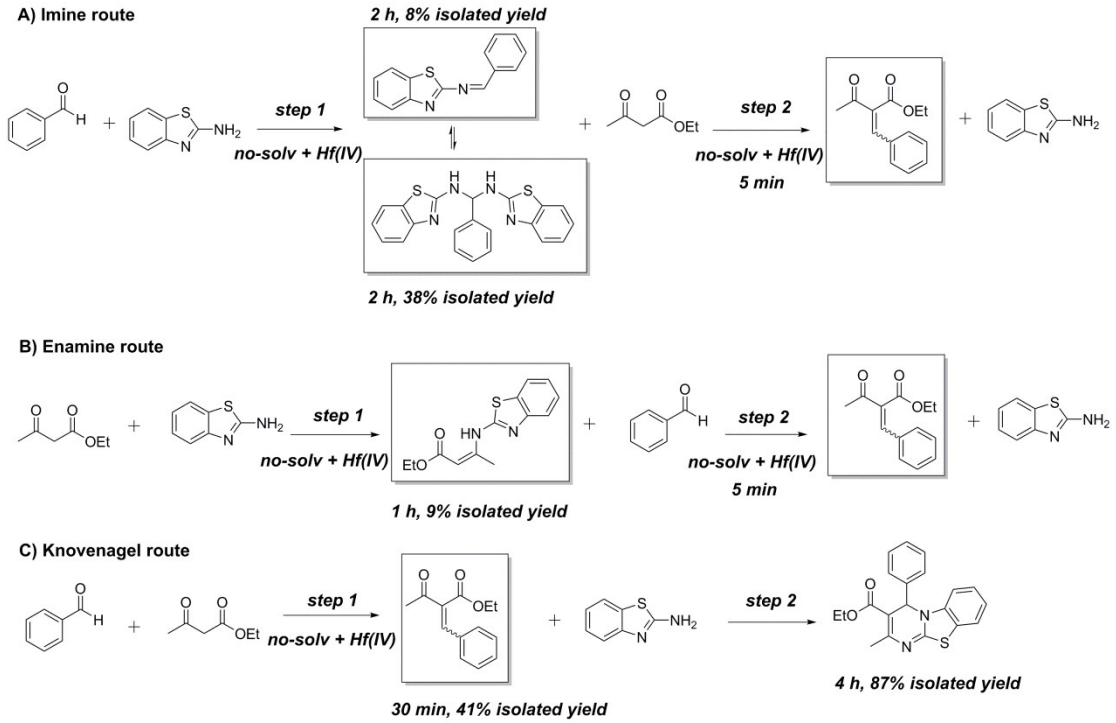

Fig. S1 Experimental results of sequential bimolecular condensation reactions.

The above experimental results indicate that the $Hf(OTf)_4$-catalyzed 3CR proceeds via the Knovenagel pathway possibly because the Knovenagel condensation product is the most stable intermediate among the three intermediates and it may further react with 2-aminobenzothiazole (the 3rd component) to shift the reaction equilibrium to the final product.

3.3 Proposed reaction mechanism

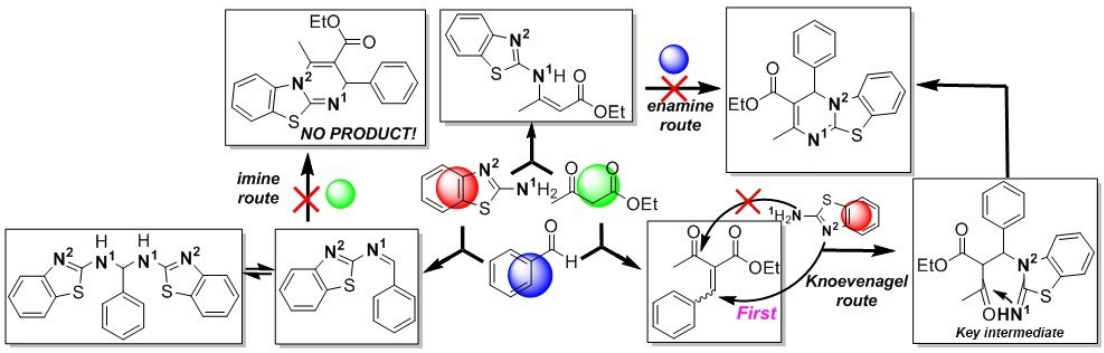

Fig. S2 Proposed mechanism for $Hf(OTf)_4$-catalyzed 3CR synthesis of **PBT-1**.

3.4 Effect of different substrates on $Hf(OTf)_4$-catalyzed 3CR

PBT-A series:

1) Either electron-donating (**A1-A3**) or electron-withdrawing (**A4**) groups on the *p*-position of benaldehyde have limited effect on the reaction yield.

2) The presence of the two substituents on the *m*-positions of benzaldehyde (**A5-A6**) makes the reactions less effective possibly due to the elevated steric hindrance.

3) The replacement of benzaldehyde with other aryl aldehydes (**A7-A8**) shows limited effect on the yield. But the propylaldehyde (**A9**) affords the corresponding product in a much lower yield possibly due to its high volatility.

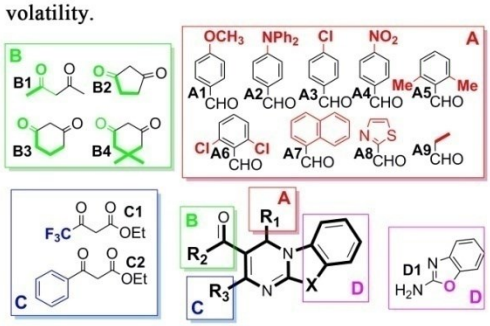

PBT-B and **PBT-C** series:

1) The 1,3-diketone substrates (**B1-B4**) exhibit comparable reactivity to ethyl acetoacetate. The more rigid 1,3-cyclopentanedione's (**B2**) reaction rate is even faster.

2) When acetoacetate is replaced by trifluoroacetoacetate (**C1**) and benzoylacetate (**C2**), the reaction yields are lowered. The reaction rate of benzoylacetate is much slower (24 h) possibly due to the presence of the aryl ketone.

PBT-D series:

The reactivity of 2-aminobenzoxazole (**D1**) is not as good as that of 2-aminobenzthiazole and affords the corresponding product in a lowered yield and prolonged reaction time.

Fig. S3 Influence of different substituents on reaction yield

4. Photophysical data

4.1 Absorption and fluorescence spectra of PBT AIEgens in solution and solid state

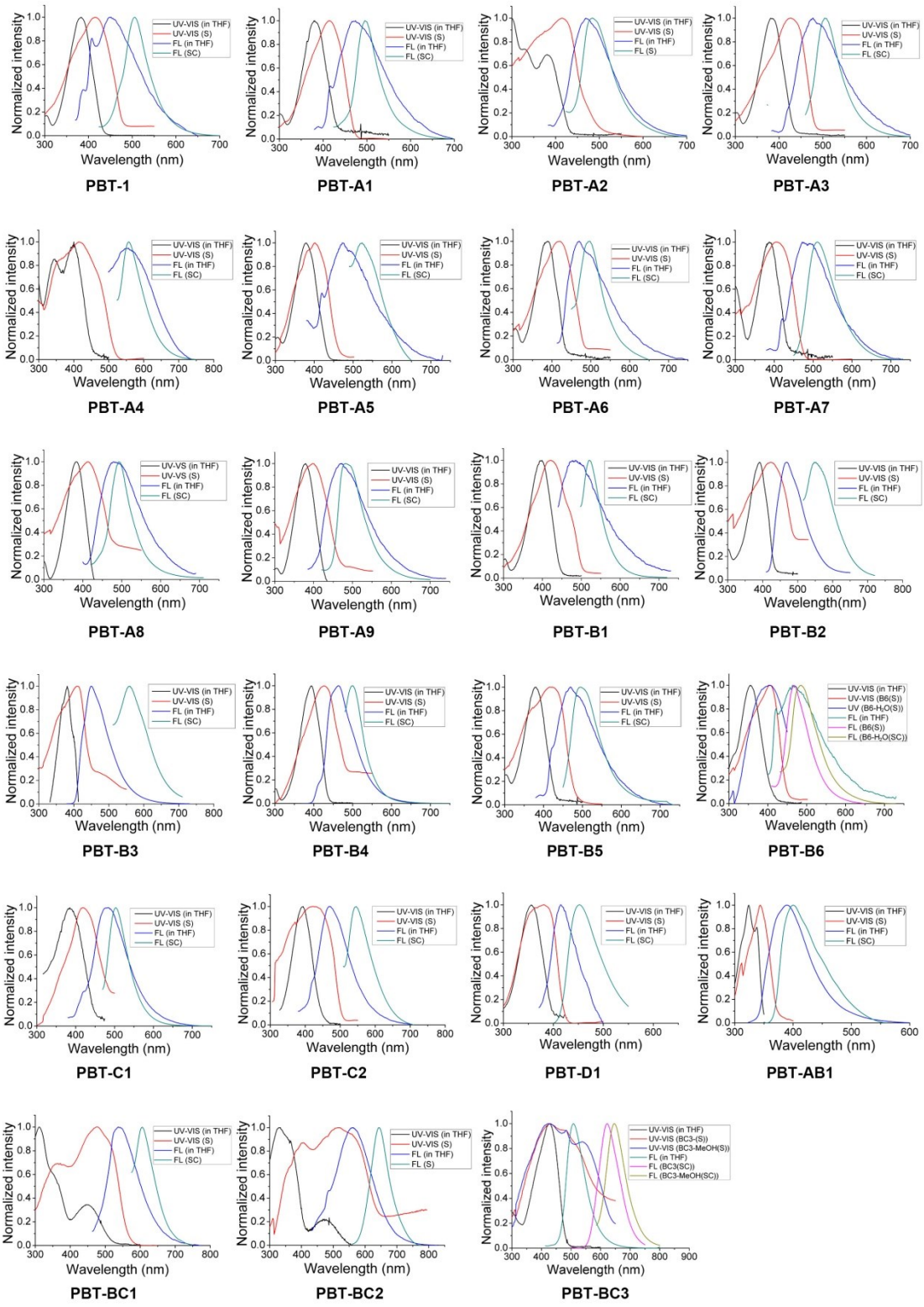

Fig. S4 UV-Vis and PL spectra of PBT AIEgens in solution ([PBT]=5×10^{-5} M) and solid state ((S): amorphous solid; (SC): single crystal)

4.2 Absorption and fluorescence spectra of PBT-AB1 in different organic solvents

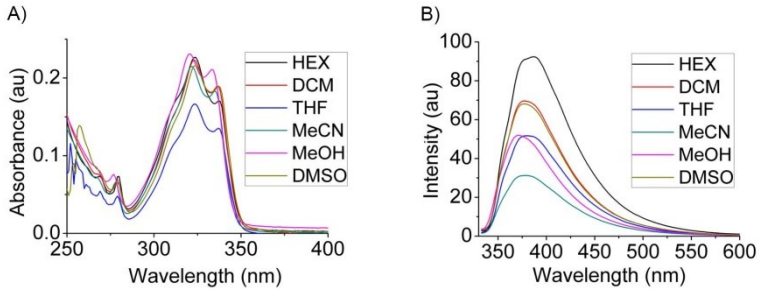

Fig. S5 UV-Vis and PL spectra of **PBT-AB1** in different organic solvents ([**PBT-AB1**]=2×10^{-5} M for UV-Vis; 5×10^{-5} M for PL)

5. Theoretical calculations

5.1 Electronic structures of PBT AIEgens

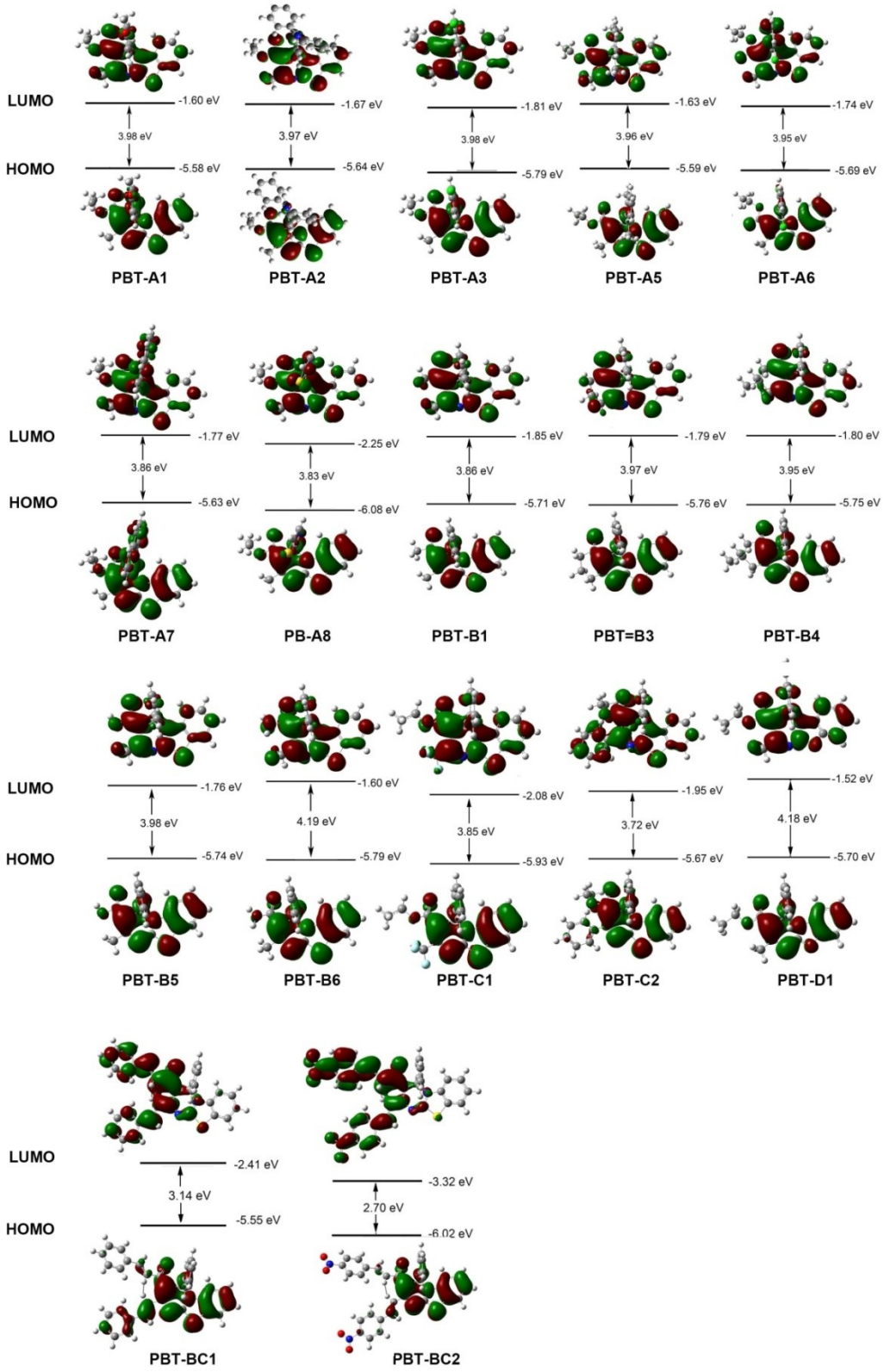

Fig. S6 Molecular orbital amplitude plots of HOMO and LUMO energy levels of PBT AIEgens calcuated by using B3LYP/6-31G(d) basis set

5.2 Vertical excitation calculations of representative PBT AIEgens

Table S2 Selected parameters for the vertical excitation of **PBT-1** obtained by TDDFT calculation at B3LYP/6-31G(d) level

Electronic transition	Energy, eV/λ nm	f^a	Composition[b]	CI[c]
S0→S1	3.36/368	0.3687	H→L	0.70281
S0→S2	4.36/284	0.0297	H→L+1	0.62094
S0→S3	4.48/277	0.0047	H→L+2	0.52004

[a]Oscillator strength. [b]H, HOMO (highest occupied molecular orbital) and L, LUMO (lowest unoccupied molecular orbital). [c]Coefficient of wavefunction.

Table S3 Selected parameters for the vertical excitation of **PBT-A4** obtained from TDDFT calculation at B3LYP/6-31G(d) level

Electronic transition	Energy, eV/λ nm	f^a	Composition[b]	CI[c]
$S_0 \rightarrow S_1$	2.54/489	0.0224	H→L	0.70330
$S_0 \rightarrow S_2$	3.47/357	0.3769	H→L+1	0.69999
$S_0 \rightarrow S_3$	3.77/329	0.0081	H-1→L	0.70120

[a]Oscillator strength. [b]H, HOMO (highest occupied molecular orbital) and L, LUMO (lowest unoccupied molecular orbital). [c]Coefficient of wavefunction.

Table S4 Selected parameters for the vertical excitation of **PBT-AB1** obtained from TDDFT calculation at B3LYP/6-31G(d) level

Electronic transition	Energy, eV/λ nm	f^a	Composition[b]	CI[c]
$S_0 \rightarrow S_1$	4.12/301	0.2566	H→L	0.69455
$S_0 \rightarrow S_2$	4.78/259	0.0277	H-1→L	0.59439
$S_0 \rightarrow S_3$	4.80/258	0.0000	H-3→L	0.68240

[a]Oscillator strength. [b]H, HOMO (highest occupied molecular orbital) and L, LUMO (lowest unoccupied molecular orbital). [c]Coefficient of wavefunction.

Table S5 Selected parameters for the vertical excitation of **PBT-BC3** obtained from TDDFT calculation at B3LYP/6-31G(d) level

Electronic transition	Energy, eV/λ nm	f^a	Composition[b]	CI[c]
$S_0 \rightarrow S_1$	2.81/442	0.8373	H→L	0.64996
$S_0 \rightarrow S_2$	3.20/388	0.1158	H-1→L	0.60793
$S_0 \rightarrow S_3$	3.34/371	0.0231	H-2→L	0.65070

[a]Oscillator strength. [b]H, HOMO (highest occupied molecular orbital) and L, LUMO (lowest unoccupied molecular orbital). [c]Coefficient of wavefunction.

5.3 Quantitative correlation between rotation of ester and distortion of pyrimidine ring

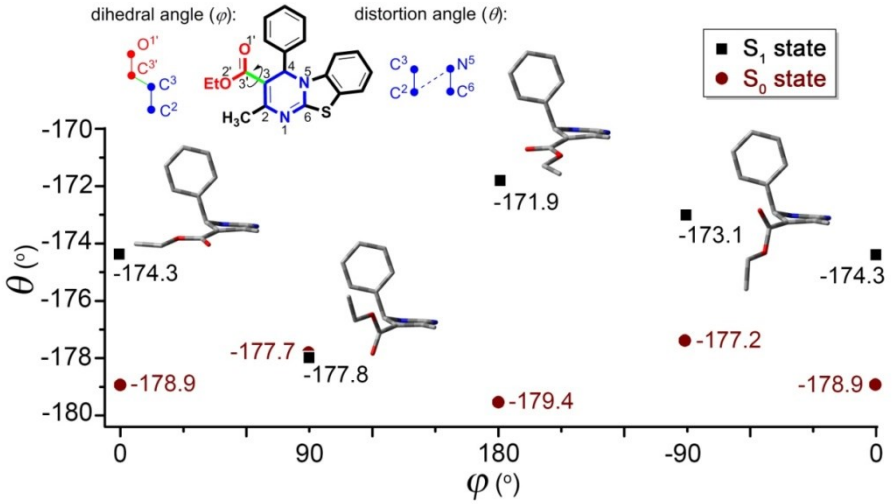

Fig. S7 Optimized geometries and distortion angles (θ) of **PBT-1** in S_1 state at different dihedral angles: (φ=0°, 90°, 180°, -90°). Distortion angles (θ) of **PBT-1** in S_0 state are also presented for comparison. H atoms and benzothiazole moiety are omitted for clarity.

6. Crystallographic analysis

6.1 Crystal data of PBT single crystals

Table S6 ORTEP drawings, CCDC numbers, and crystal data of PBT AIEgens

	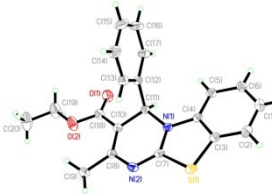	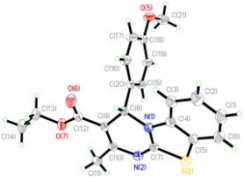	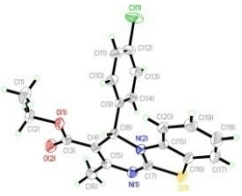
	PBT-1	**PBT-A1**	**PBT-A3**
CCDC Number		**2083529**	**2082831**
Fomula	$C_{20}H_{18}N_2O_2S$	$C_{21}H_{20}N_2O_3S$	$C_{20}H_{17}ClN_2O_2S$
Fomula weight	350.42	380.45	384.86
Temperature (K)	296(2)	296(2)	296(2)
Crystal system	Monoclinic	Monoclinic	Orthorhombic
Space group	P21/n	P21/n	Pbcn
Unit cell dimensions			
a (Á)	10.4730(11)	8.3164(9)	19.8446(18)
b (Á)	9.6593(10)	26.101(3)	8.2197(8)
c (Á)	17.367(2)	17.840(2)	23.165(2)
α (º)	90	90	90
β (º)	96.245(2)	101.630(2)	90
γ (º)	90	90	90
Volume ($Á^3$)	1746.5(3)	3792.9(7)	3778.6(6)
Z	4	4	8
Density(calcd)(g/cm^3)	1.333	1.332	1.353
Goodness-of-fit on F^2	1.029	0.991	1.029
Final R indices [I/2σ(I)]			
R1	0.0410	0.0541	0.0466
w R2	0.1070	0.1409	0.1218
R indices (all data)			
R1	0.0550	0.1106	0.1054
w R2	0.1189	0.1745	0.1674

		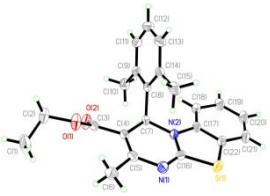	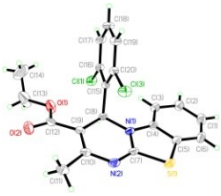
	PBT-A4	**PBT-A5**	**PBT-A6**
CCDC Number	**2083684**	**2083669**	**2083672**
Fomula	$C_{20}H_{17}N_3O_4S$	$C_{22}H_{22}N_2O_2S$	$C_{22}H_{22}N_2O_2S$
Fomula weight	395.42	378.47	378.47
Temperature (K)	296(2)	296(2)	296(2)
Crystal system	Orthorhombic	Triclinic	Triclinic
Space group	Pbcn	P-1	P-1
Unit cell dimensions			
a (Á)	19.861(4)	9.4948(18)	9.4948(18)
b (Á)	8.0720(17)	9.5464(19)	9.5464(19)
c (Á)	23.601(5)	11.480(2)	11.480(2)
α (º)	90	103.093(2)	103.093(2)
β (º)	90	109.576(2)	109.576(2)
γ (º)	90	91.166(2)	91.166(2)
Volume (Á^3)	3783.6(14)	949.7(3)	949.7(3)
Z	8	2	2
Density(calcd)(g/cm^3)	1.388	1.324	1.324
Goodness-of-fit on F^2	0.934	1.057	1.057
Final R indices [I/2σ(I)]			
R1	0.0558	0.0547	0.0547
w R2	0.1410	0.1548	0.1548
R indices (all data)			
R1	0.1196	0.0700	0.0700
w R2	0.1804	0.1708	0.1708

	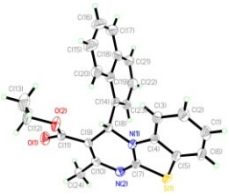	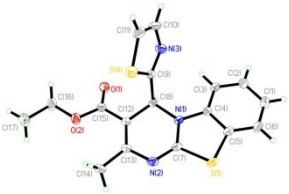	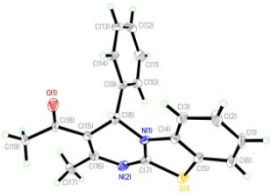
	PBT-A7	**PBT-A8**	**PBT-B1**
CCDC Number	**2083676**	**2083671**	**2083674**
Fomula	$C_{17}H_{15}N_3O_2S_2$	$C_{20}H_{16}Cl_2N_2O_2S$	$C_{19}H_{16}N_2OS$
Fomula weight	357.44	419.31	320.40
Temperature (K)	296(2)	296(2)	296(2)
Crystal system	Monoclinic	Monoclinic	Orthorhombic
Space group	P2(1)/c	P2(1)/c	Pca21
Unit cell dimensions			
a (Á)	10.374(11)	9.8686(11)	21.331(3)
b (Á)	9.403(10)	17.2210(19)	9.7246(13)
c (Á)	18.919(16)	11.4936(13)	7.5317(10)
α (º)	90	90	90
β (º)	116.50(4)	106.030(2)	90
γ (º)	90	90	90
Volum (Á^3)	1652(3)	1877.4(4)	1562.4(4)
Z	8	4	4
Density(calcd)(g/cm^3)	1.438	1.484	1.362
Goodness-of-fit on F^2	1.043	0.962	1.117
Final R indices[I/2σ(I)]			
R1	0.0410	0.0425	0.1192
w R2	0.1083	0.1040	0.3310
R indices (all data)			
R1	0.0525	0.0643	0.1228
w R2	0.1178	0.1179	0.3346

	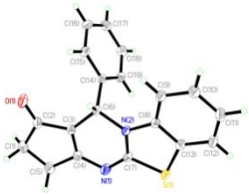	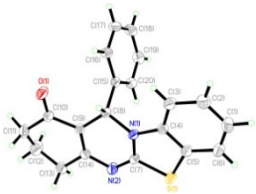	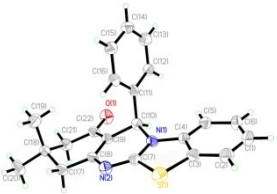
	PBT-B2	**PBT-B3**	**PBT-B4**
CCDC Number	**2083670**	**2083682**	**2083673**
Fomula	$C_{19}H_{14}N_2OS$	$C_{20}H_{16}N_2OS$	$C_{22}H_{20}N_2O_1S$
Fomula weight	318.38	332.41	360.46
Temperature (K)	296(2)	296(2)	296(2)
Crystal system	Orthorhombic	Orthorhombic	triclinic
Space group	Pbca	Pbca	P-1
Unit cell dimensions			
a (Á)	7.8993(5)	8.0329(6)	9.482(3)
b (Á)	19.1467(13)	19.2813(13)	9.587(3)
c (Á)	19.7329(14)	20.7588(14)	23.807(7)
α (º)	90	90	90
β (º)	90	90	90
γ (º)	90	90	118.997(5)
Volume (Á^3)	2984.5(3)	3215.2(4)	1892.8(10)
Z	8	8	2
Density(calcd)(g/cm^3)	1.417	1.373	1.265
Goodne ss-of-fit on F^2	1.005	1.022	0.870
Final R indices [I/2σ(I)]			
R1	0.0382	0.0487	0.0709
w R2	0.0934	0.1272	0.1504
R indices (all data)			
R1	0.0551	0.0717	0.1935
w R2	0.1045	0.1437	0.1884

	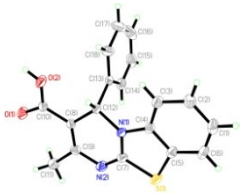	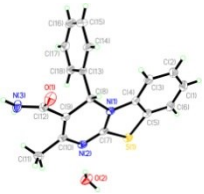	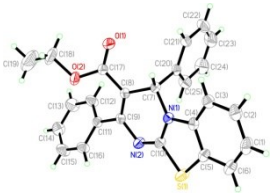
	PBT-B5	**PBT-B6-H_2O**	**PBT-C1**
CCDC Number	**2083675**	**2083677**	**2083681**
Fomula	$C_{18}H_{14}N_2O_2S$	$C_{18}H_{17}N_3O_2S$	$C_{20}H_{15}F_3N_2O_2S$
Fomula weight	322.37	339.40	404.40
Temperature (K)	296(2)	296(2)	296(2)
Crystal system	Triclinic	Triclinic	Monoclinic
Space group	P -1	P -1	P2(1)/c
Unit cell dimension			
a (Á)	7.5403(9)	9.0493(9)	11.749(4)
b (Á)	8.8750(10)	9.3379(9)	17.194(6)
c (Á)	12.4650(14)	9.6639(9)	9.398(3)
α (º)	72.2060(10)	86.8130(10)	90
β (º)	81.9390(10)	85.7700(10)	101.271(6)
γ (º)	77.2670(10)	82.6970(10)	90
Volume ($Á^3$)	772.33(15)	806.90(13)	1862.0(10)
Z	2	2	4
Density(calcd)(g/cm^3)	1.386	1.397	1.443
Goodness-of-fit on F^2	1.036	1.033	1.004
Final R indices [I/2σ(I)]			
R1	0.0392	0.0413	0.0590
w R2	0.1038	0.1144	0.1473
R indices (all data)			
R1	0.0497	0.0501	0.1356
w R2	0.1124	0.1217	0.2017

		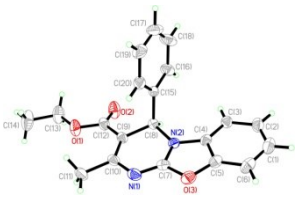	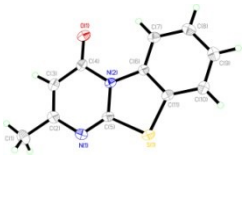
	PBT-C2	**PBT-D1**	**PBT-AB1**
CCDC Number	**2083679**	**2083680**	**2083668**
Fomula	$C_{25}H_{20}N_2O_2S$	$C_{20}H_{18}N_2O_3$	$C_{11}H_8N_2OS$
Fomula weight	412.49	334.36	216.25
Temperature (K)	296(2)	296(2)	296(2)
Crystal system	Monoclinic	Monoclinic	Monoclinic
Space group	C 2/c	P2(1)/c	P2(1)/c
Unit cell dimension			
a (Á)	29.055(3)	10.5026(15)	7.3929(11)
b (Á)	8.4317(8)	9.5898(14)	11.9385(18)
c (Á)	17.7462(17)	17.064(2)	10.8700(16)
α (º)	90	90	90
β (º)	104.768(2)	96.244(2)	99.511(2)
γ (º)	90	90	90
Volume (Á^3)	4204.0(7)	1708.5(4)	946.2(2)
Z	8	4	4
Density(calcd)(g/cm^3)	1.303	1.300	1.518
Goodness-of-fit on F^2	1.020	1.001	1.028
Final R indices [I/2σ(I)]			
R1	0.0487	0.0475	0.0502
w R2	0.1194	0.1318	0.1192
R indices (all data).			
R1	0.0777	0.0792	0.0929
w R2	0.1396	0.1557	0.1398

	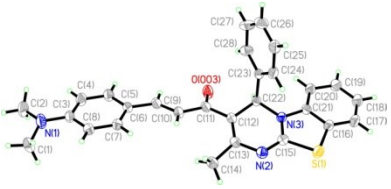	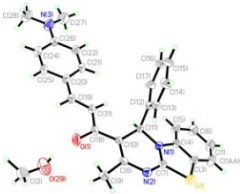
	PBT-BC3	**PBT-BC3-MeOH**
CCDC Number	**2083678**	**2083683**
Fomula	$C_{28}H_{25}N_3OS$	$C_{29}H_{29}N_3O_2S$
Fomula weight	451.57	483.61
Temperature (K)	296(2)	296(2)
Crystal system	Monoclinic	Triclinic
Space group	P 21/n	P -1
Unit cell dimensions		
a (Á)	11.1662(13)	9.644(3)
b (Á)	13.6070(16)	10.615(3)
c (Á)	16.1430(19)	12.949(4)
α (º)	90	75.074(3)
β (º)	105.550(2)	77.598(3)
γ (º)	90	89.546(3)
Volume (Á^3)	2363.0(5)	1249.5(6)
Z	4	2
Density(calcd)(g/cm^3)	1.269	1.285
Goodness-of-fit on F^2	0.933	0.947
Final R indices [I/2σ(I)]		
R1	0.0421	0.0643
w R2	0.1821	0.1821
R indices (all data)		
R1	0.0735	0.0885
w R2	0.1163	0.2104

6.2 Relationship between packing and CT properties of PBT-BC3

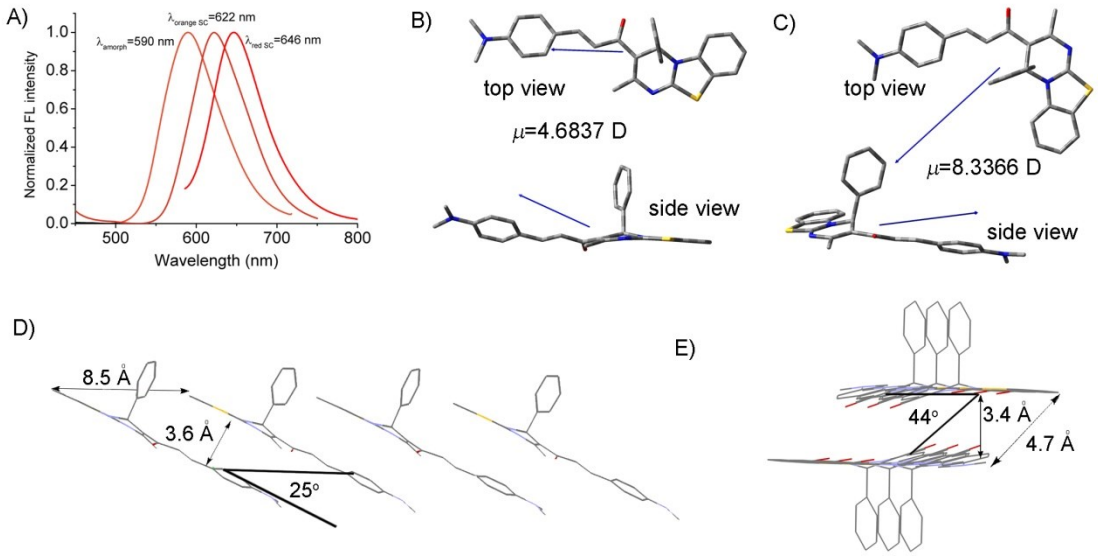

Fig. S8 Relationship between packing and CT properties of **PBT-BC3**. (A) Normalized FL spectra of amorphous, orange single crystal, and red single crystal **PBT-BC3** samples. (B) The dipole moment of **PBT-BC3**. (C) The dipole moment of **PBT-BC3-MeOH**. (D) The slip-stacked packing of **PBT-BC3**. (E) The slip-stacked packing of **PBT-BC3-MeOH**. H atoms are omitted for clarity.

6.3 Packing mode of PBT-AB1

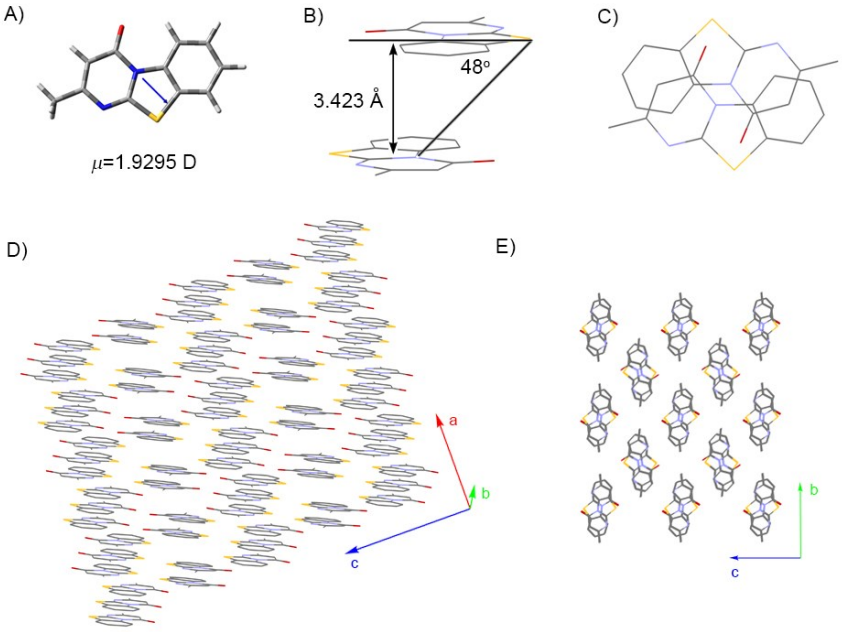

Fig. S9 Packing mode of **PBT-AB1**. (A) Dipole moment of **PBT-AB1**. (B). Side view of slip-stacked packing of two **PBT-AB1** monomers (C) Top view of slip-stacked packing of two **PBT-AB1** monomers. (D) Side view of packing alignment of **PBT-AB1**. (E) Top view of packing

alignment of **PBT-AB1**. H atoms are omitted for clarity (B–E).

7. ^{1}H and ^{13}C spectra of new PBT compounds

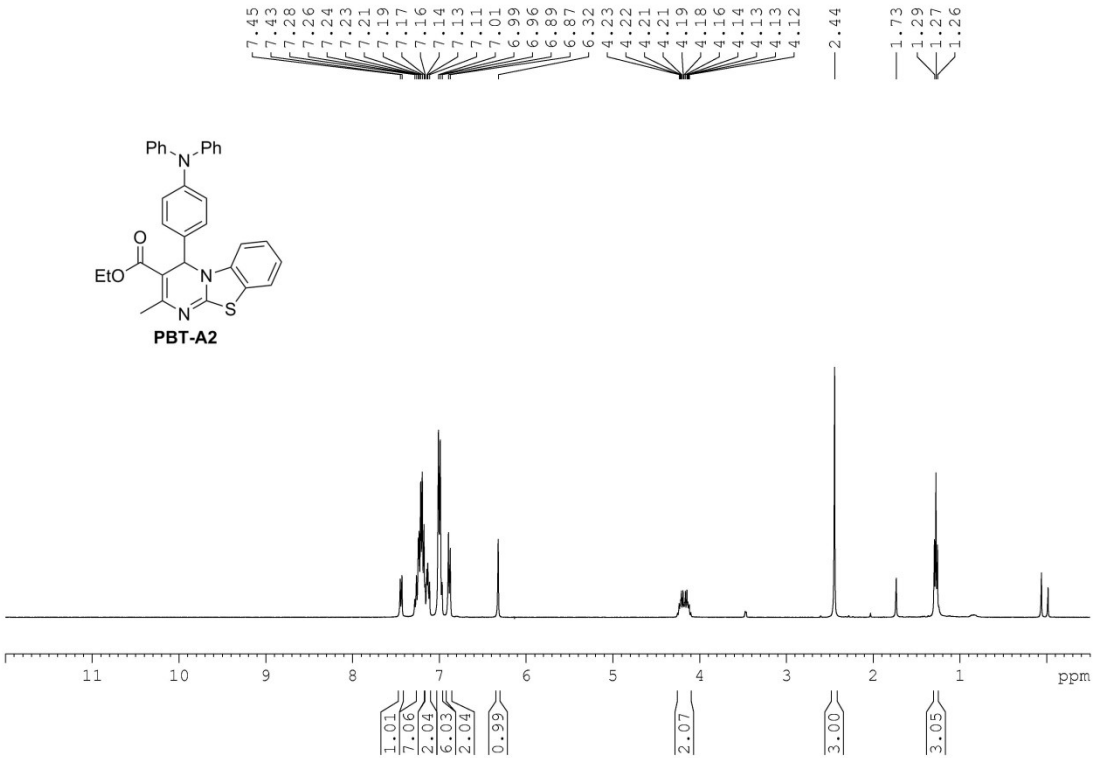

Fig. S10 ^{1}H NMR spectrum of **PBT-A2**

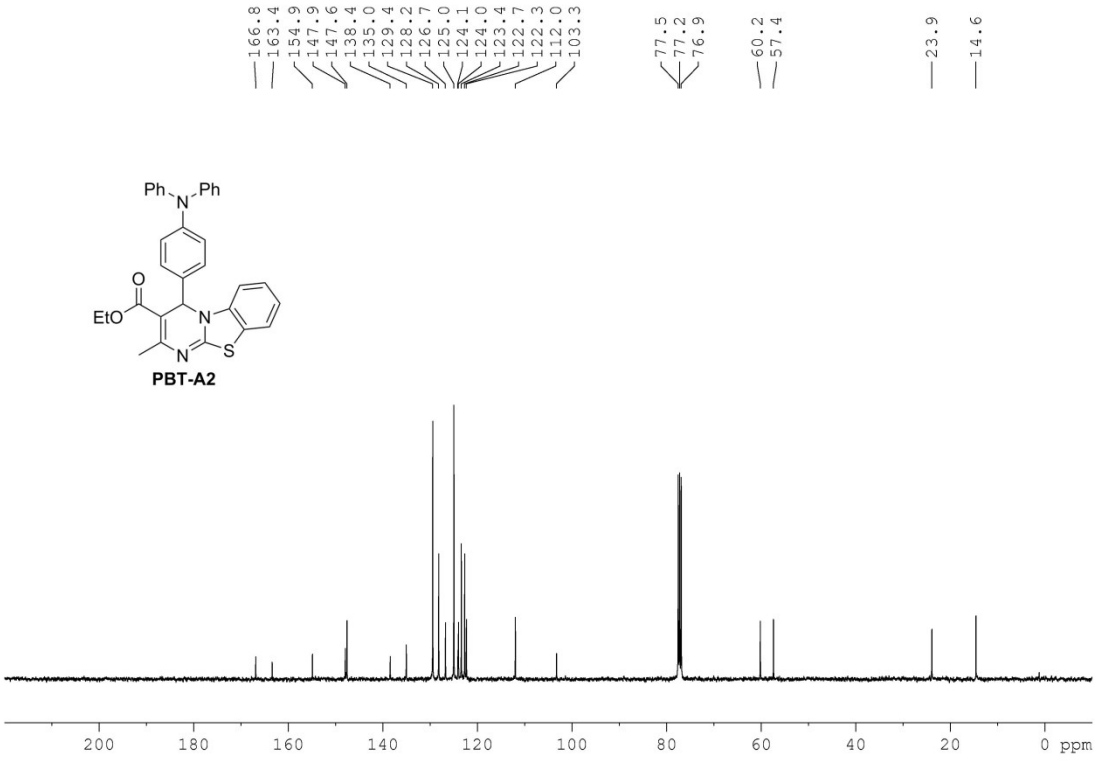

Fig. S11 ^{13}C NMR spectrum of **PBT-A2**

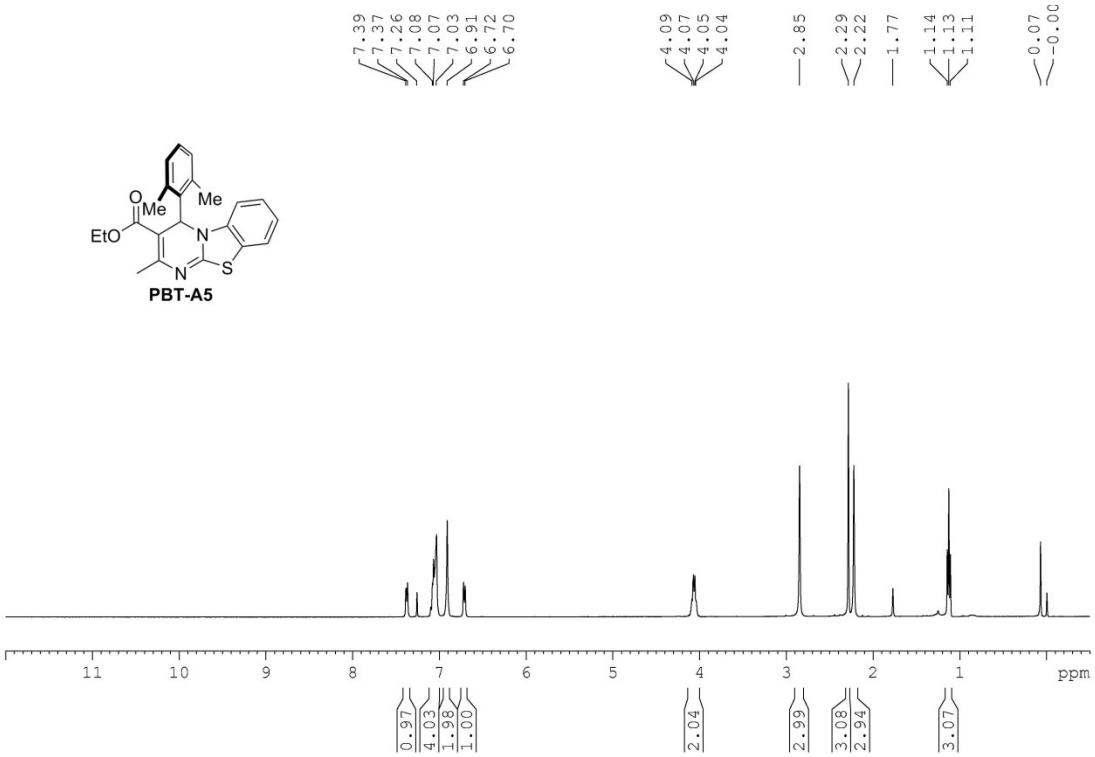

Fig. S12 [1]H NMR spectrum of **PBT-A5**

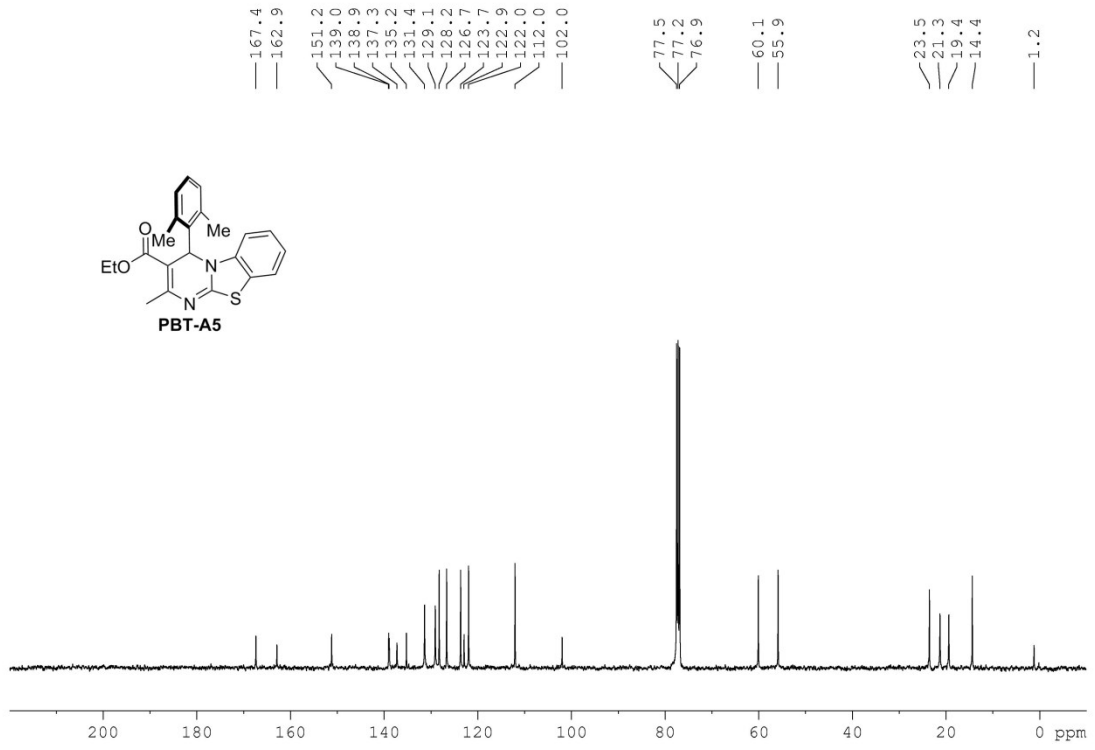

Fig. S13 [13]C NMR spectrum of **PBT-A5**

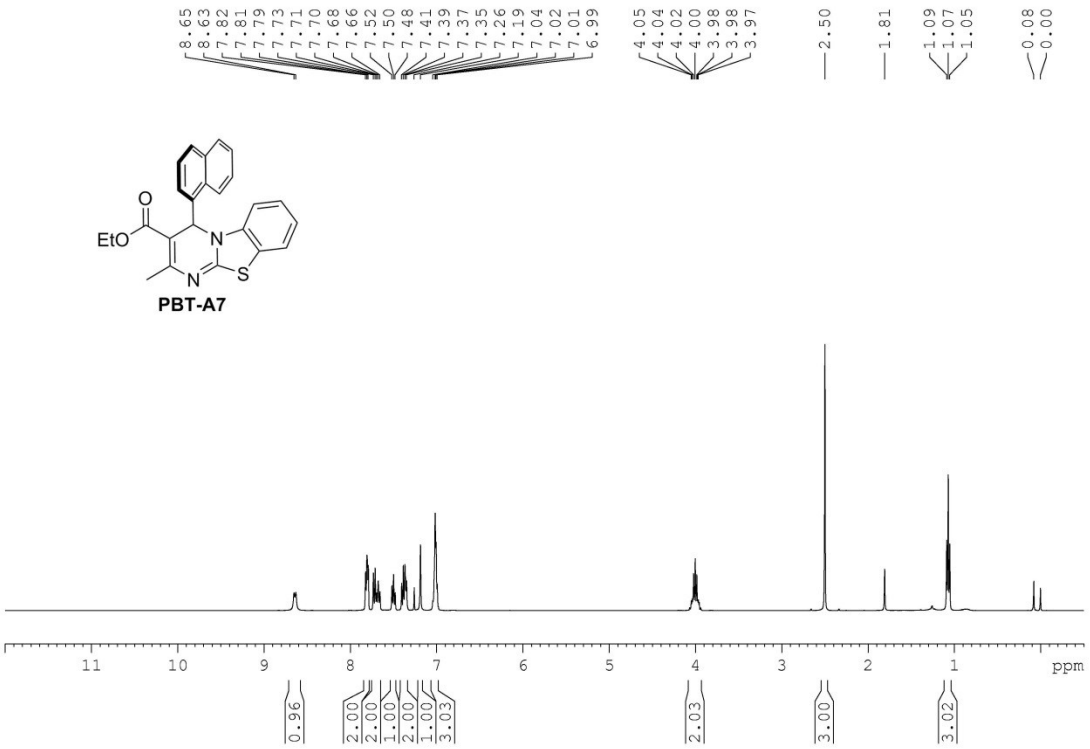

Fig. S14 ^{1}H NMR spectrum of **PBT-A7**

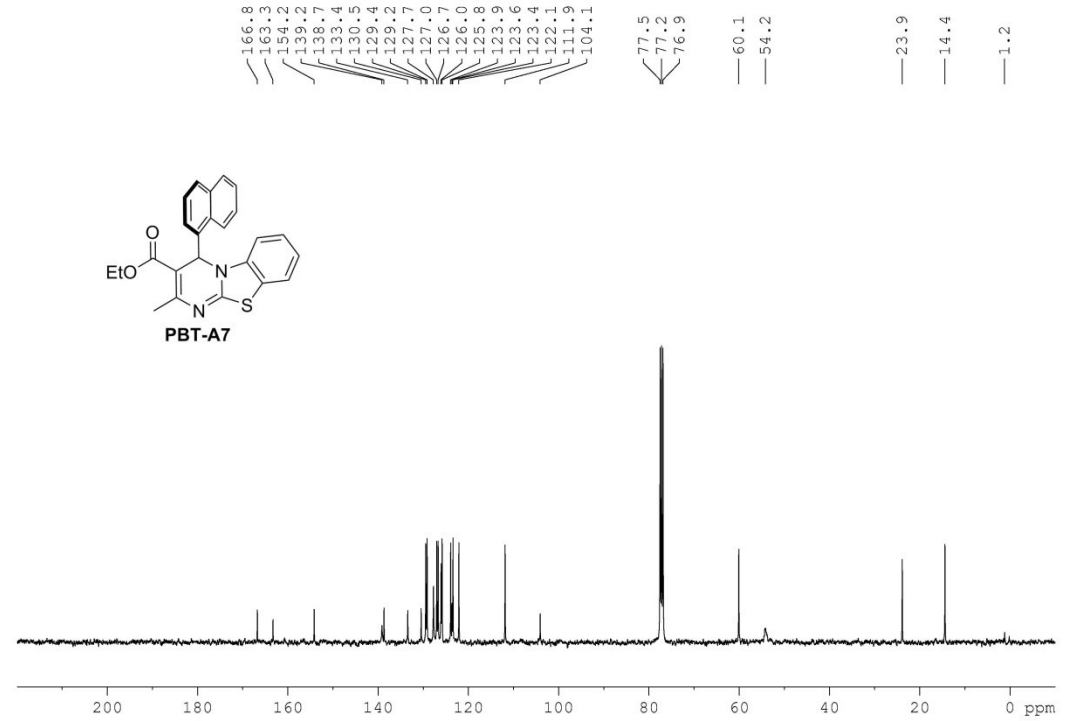

Fig. S15 ^{13}C NMR spectrum of **PBT-A7**

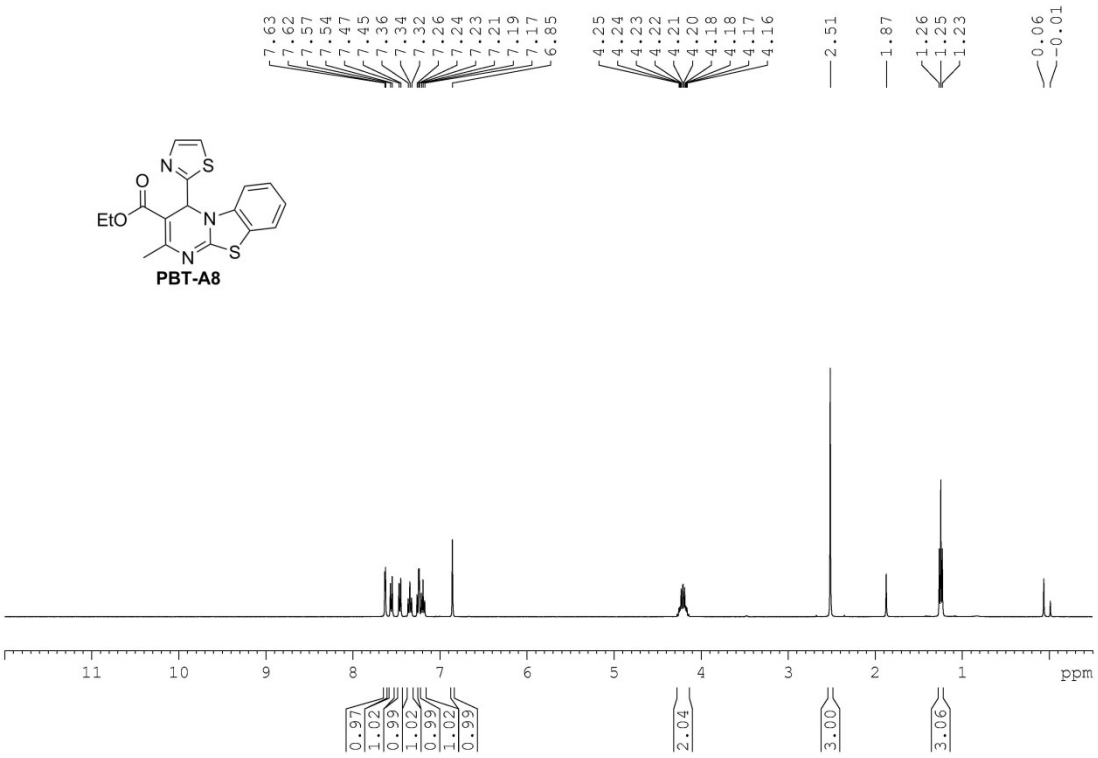

Fig. S16 ^{1}H NMR spectrum of **PBT-A8**

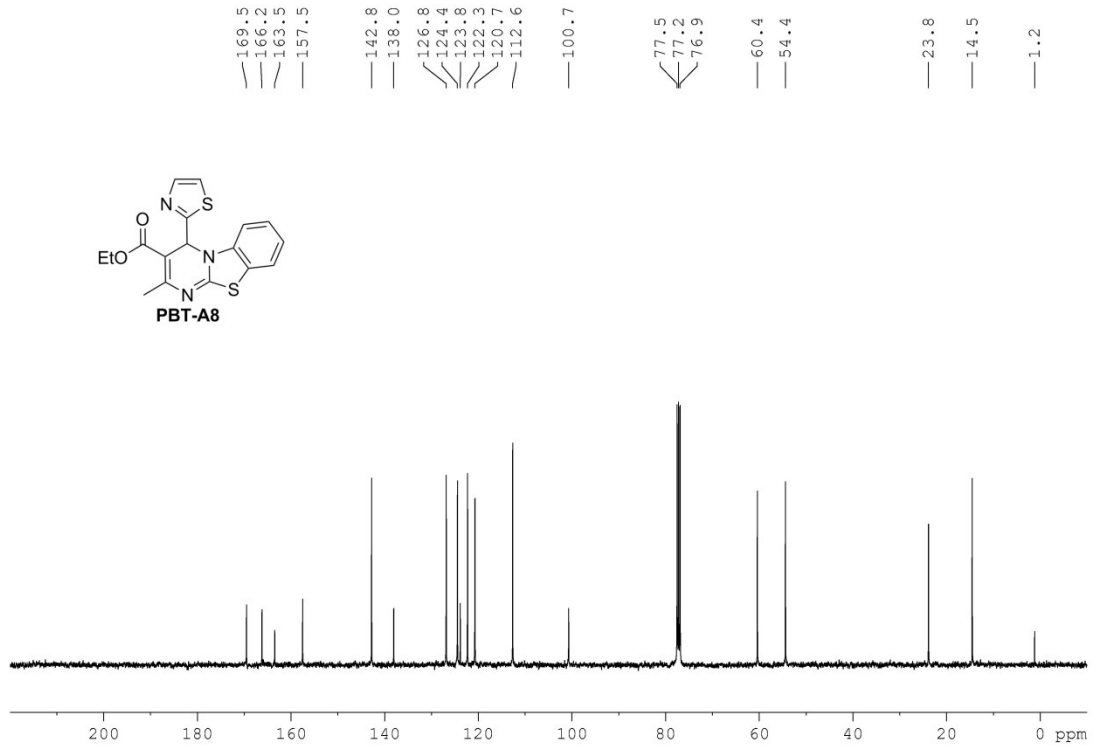

Fig. S17 ^{13}C NMR spectrum of **PBT-A8**

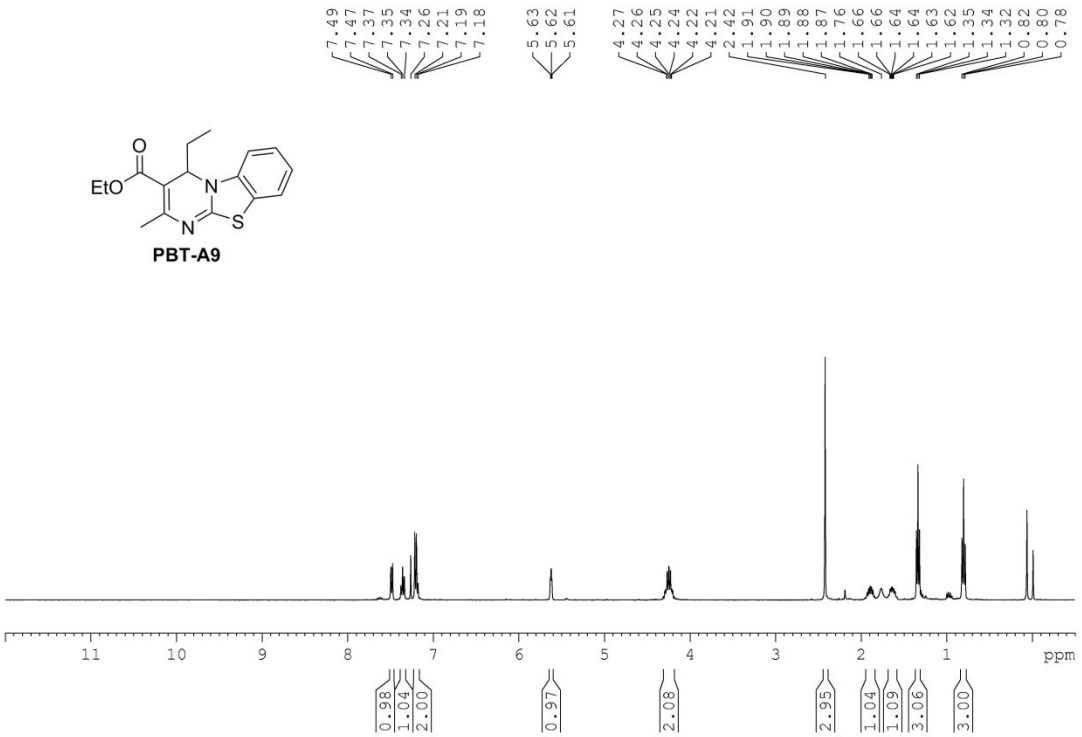

Fig. S18 ^{1}H NMR spectrum of **PBT-A9**

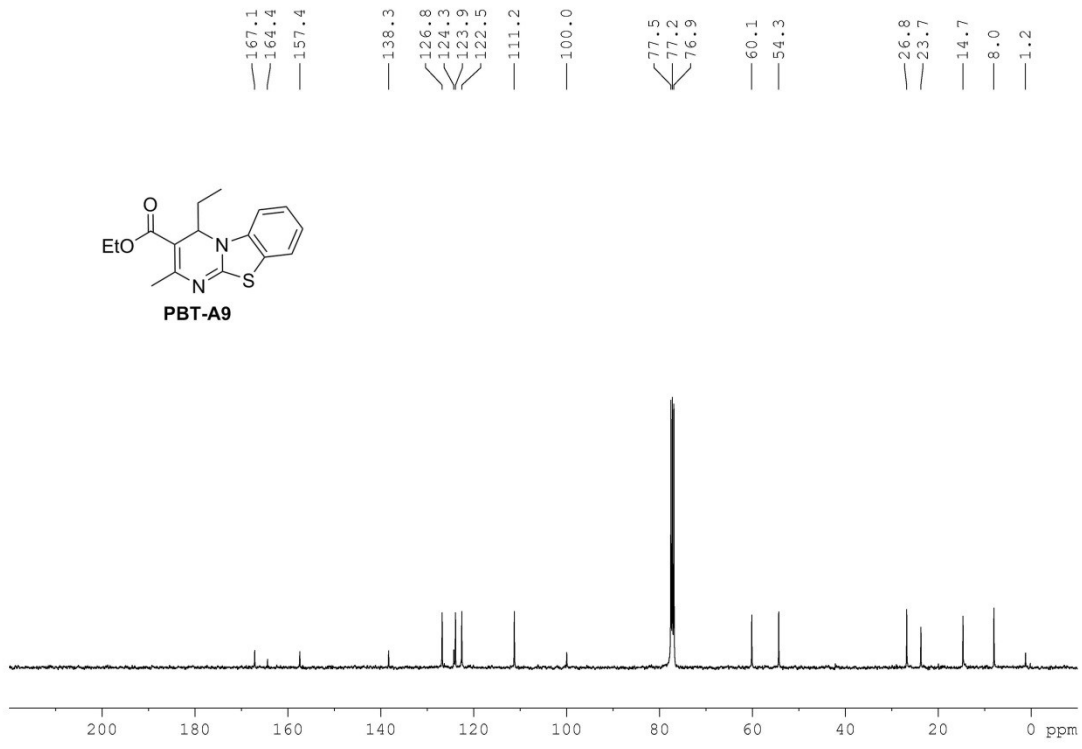

Fig. S19 ^{13}C NMR spectrum of **PBT-A9**

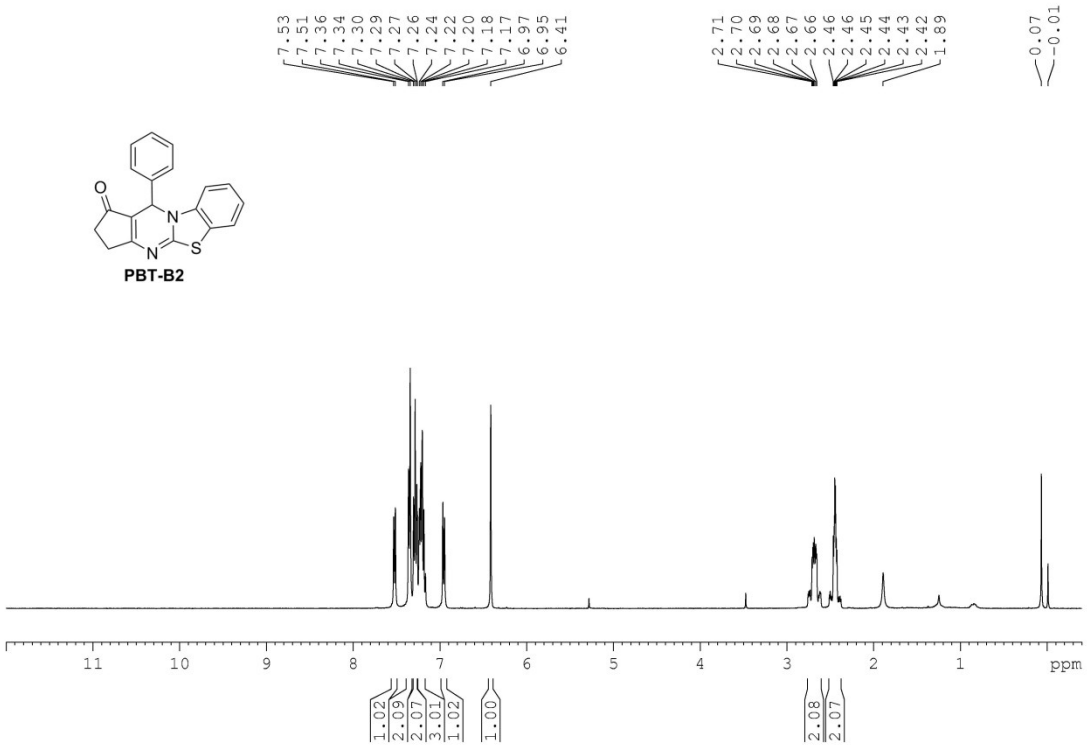

Fig. S20 ^{1}H NMR spectrum of **PBT-B2**

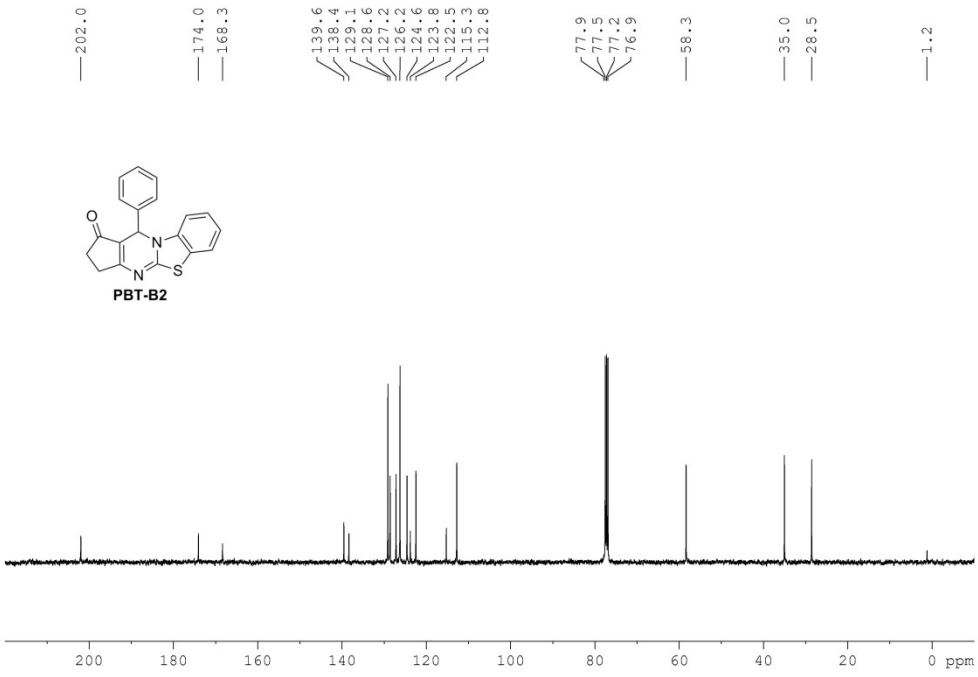

Fig. S21 ^{13}C NMR spectrum of **PBT-B2**

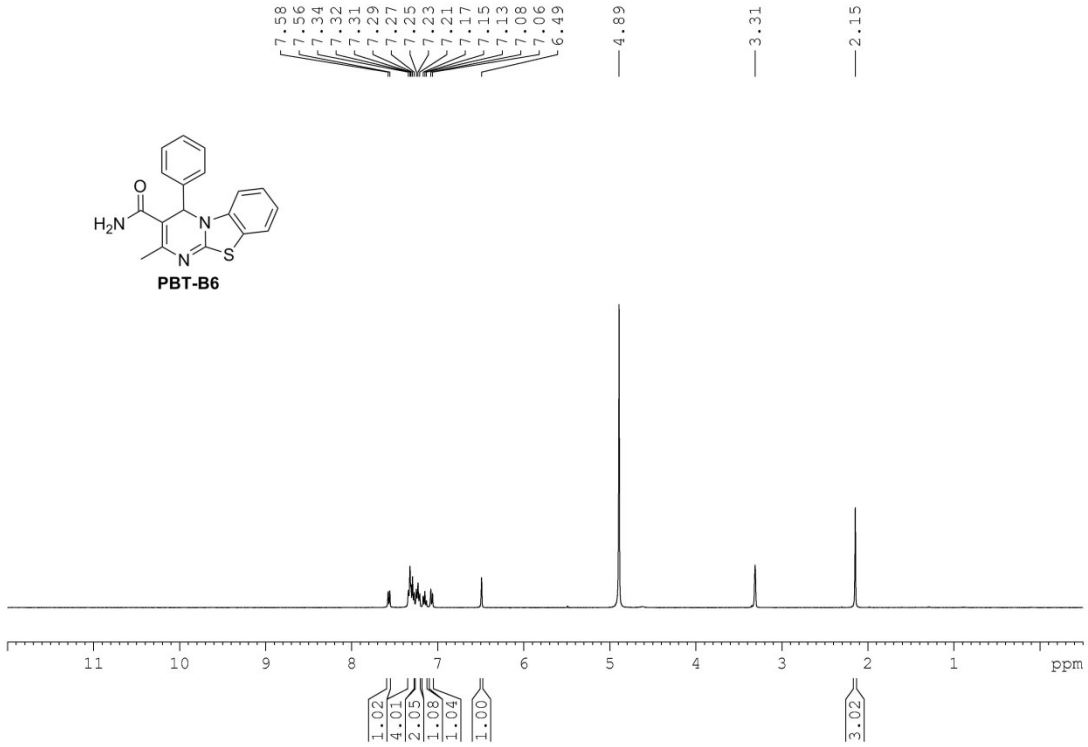

Fig. S22 ^{1}H NMR spectrum of **PBT-B6**

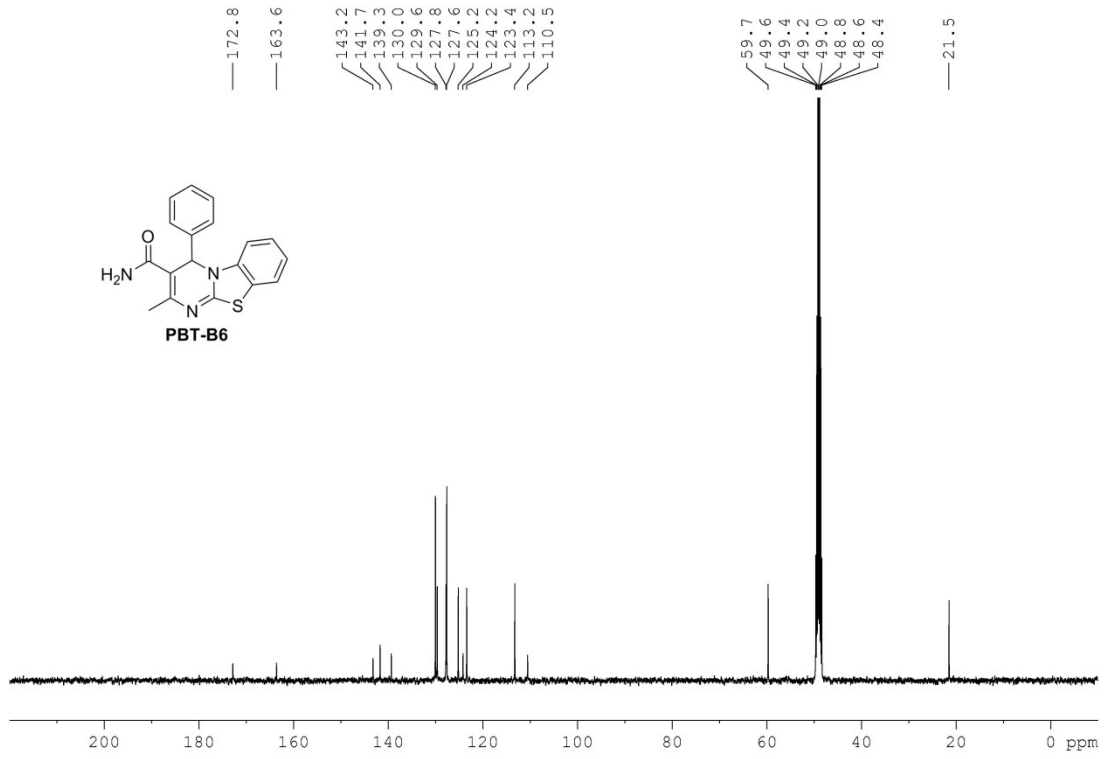

Fig. S23 ^{13}C NMR spectrum of **PBT-B6**

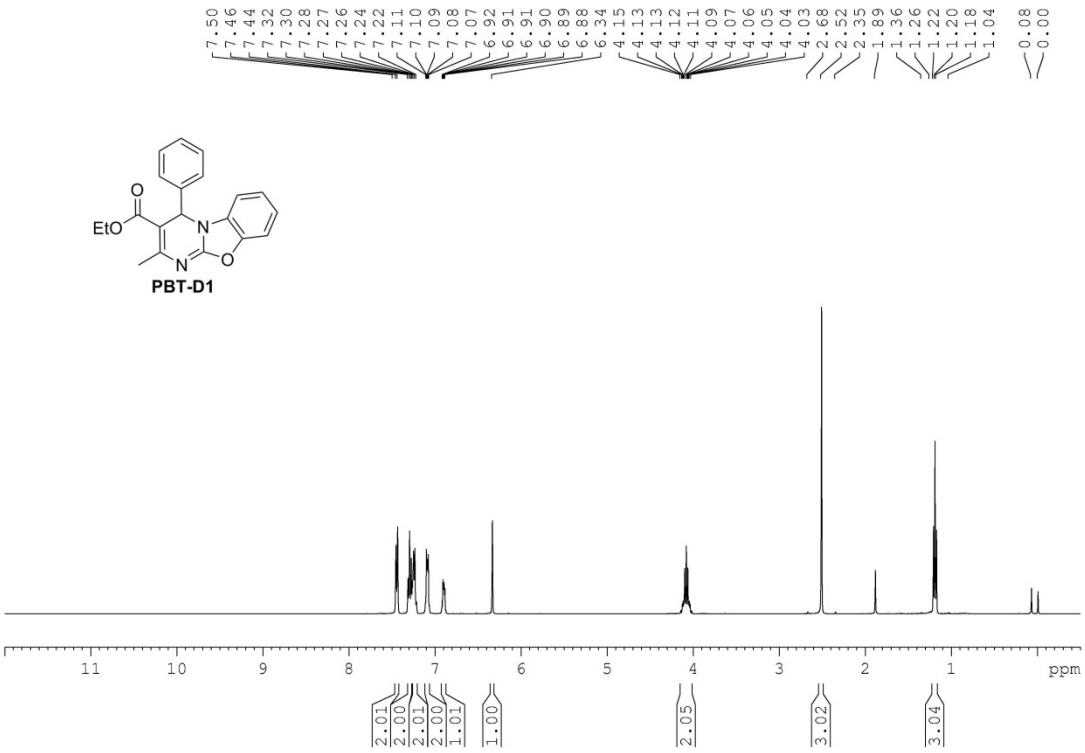

Fig. S24 ^{1}H NMR spectrum of **PBT-D1**

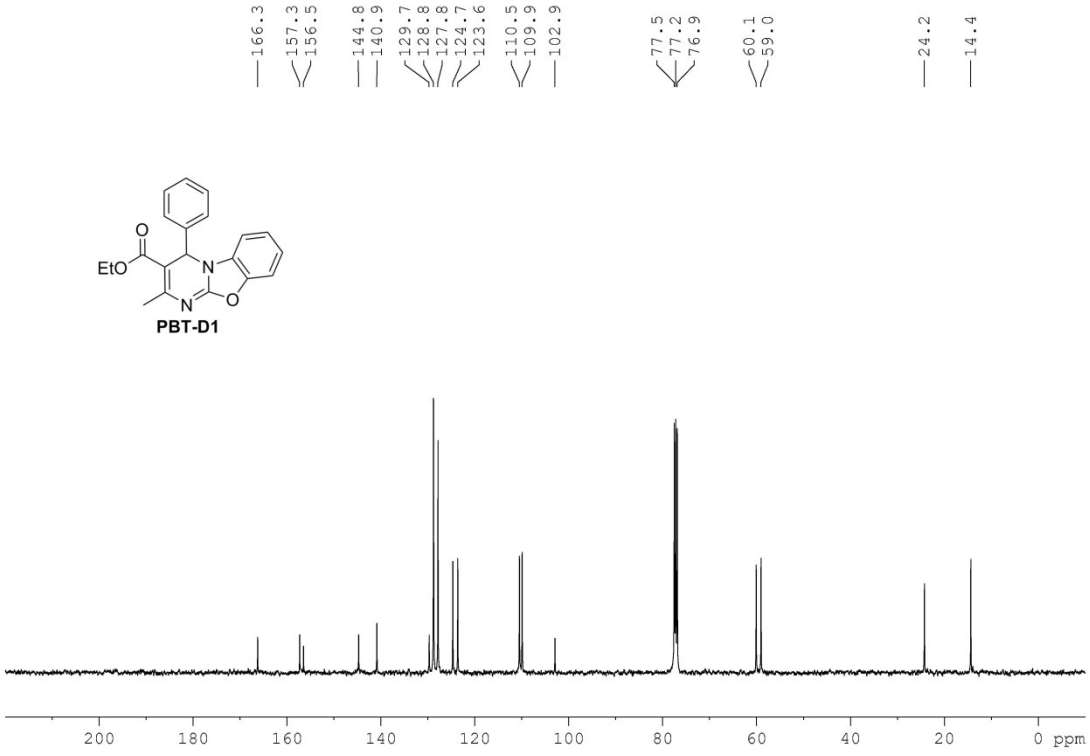

Fig. S25 ^{13}C NMR spectrum of **PBT-D1**

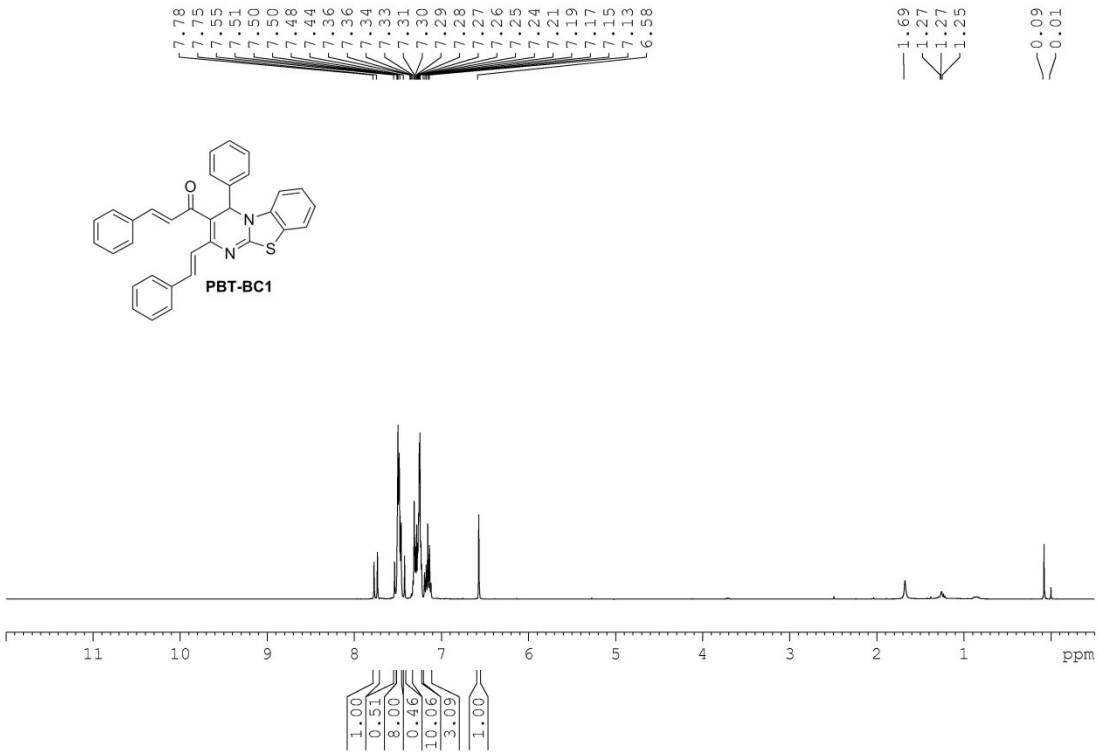

Fig. S26 ^{1}H NMR spectrum of **PBT-BC1**

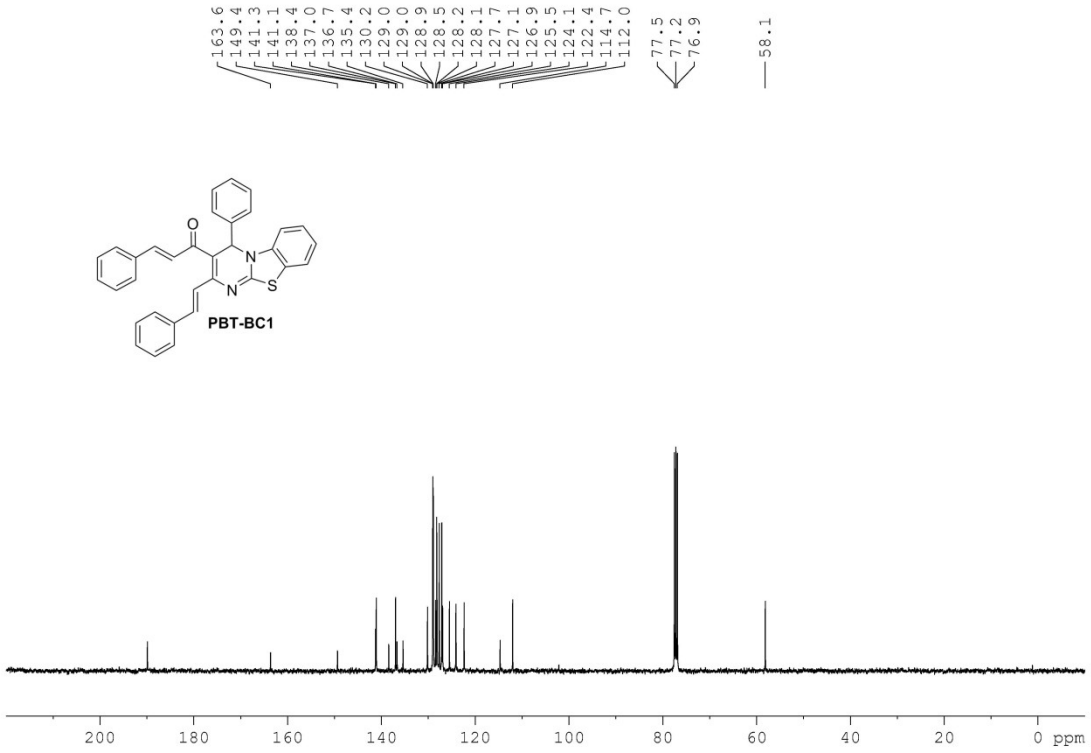

Fig. S27 ^{13}C NMR spectrum of **PBT-BC1**

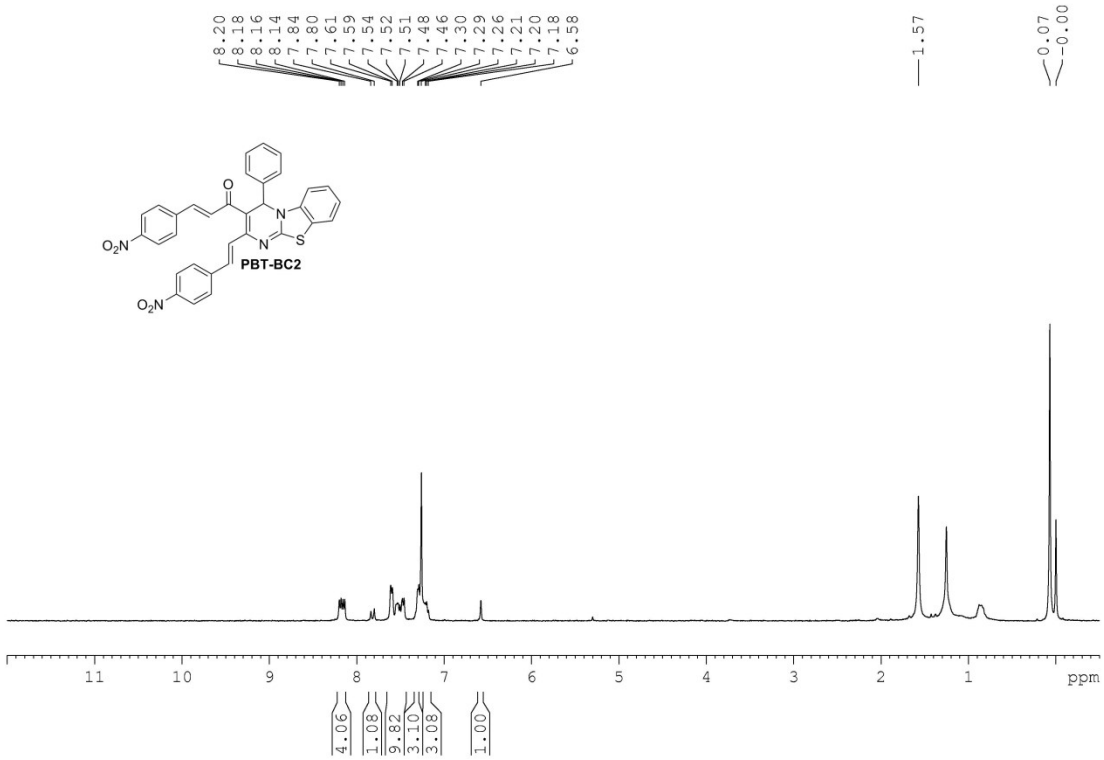

Fig. S28 ^{1}H NMR spectrum of **PBT-BC2**

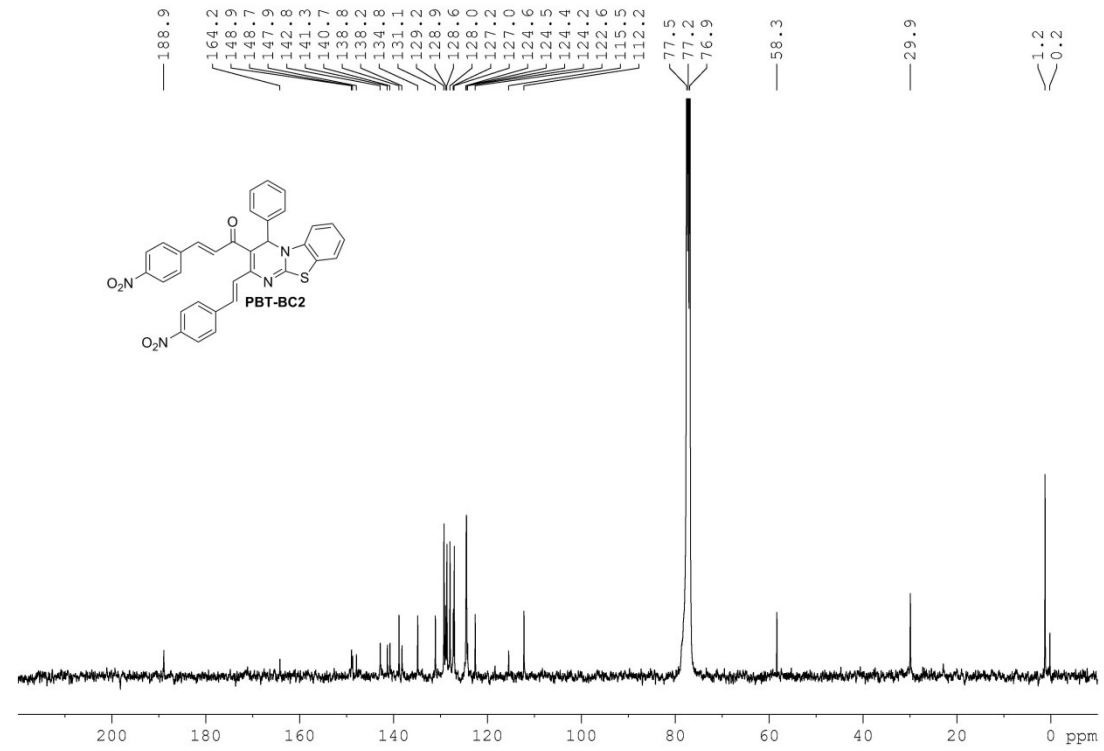

Fig. S29 ^{13}C NMR spectrum of **PBT-BC2**

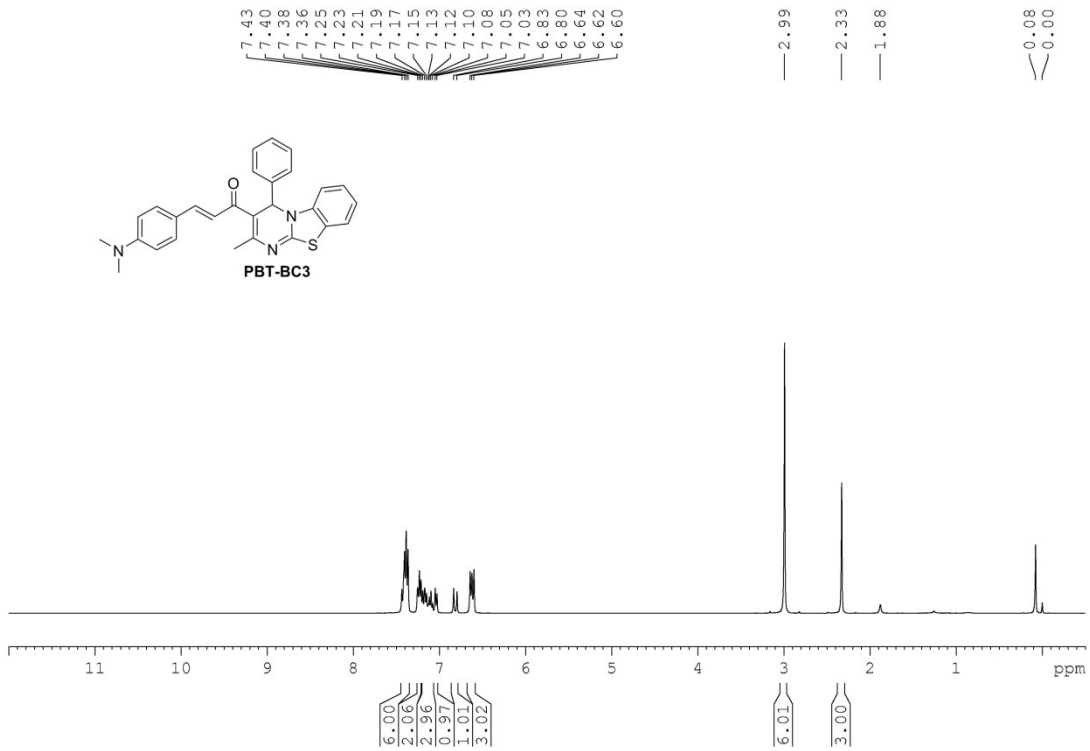

Fig. S30 ^{1}H NMR spectrum of **PBT-BC3**

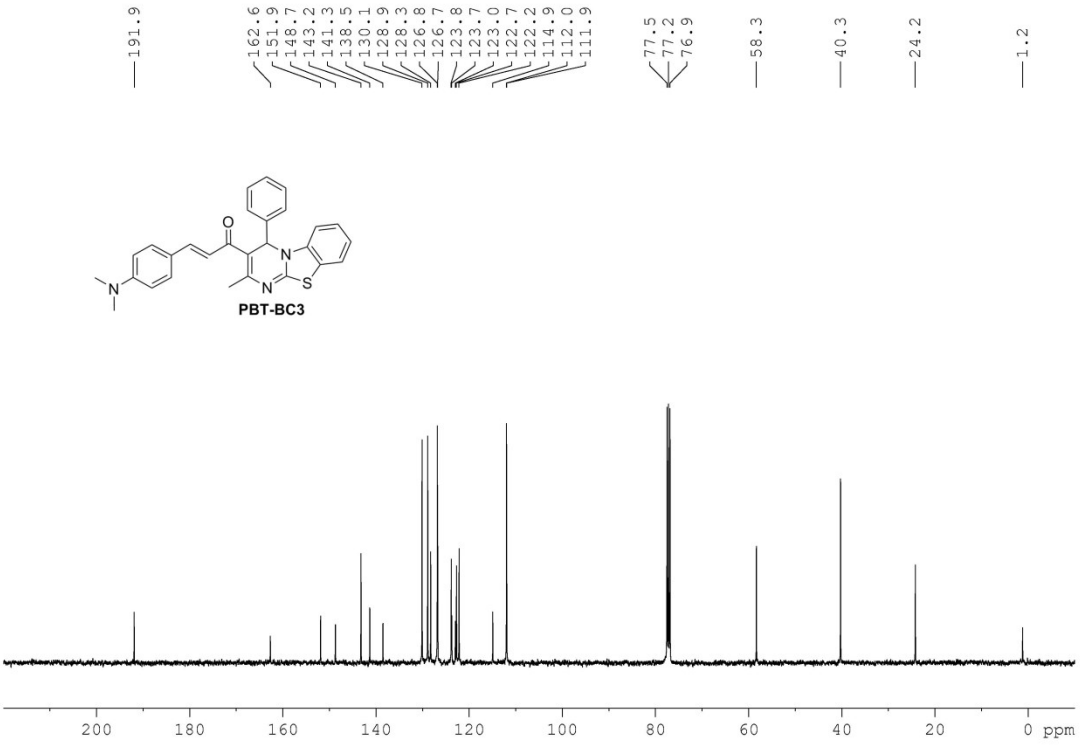

Fig. S31 ^{13}C NMR spectrum of **PBT-BC3**

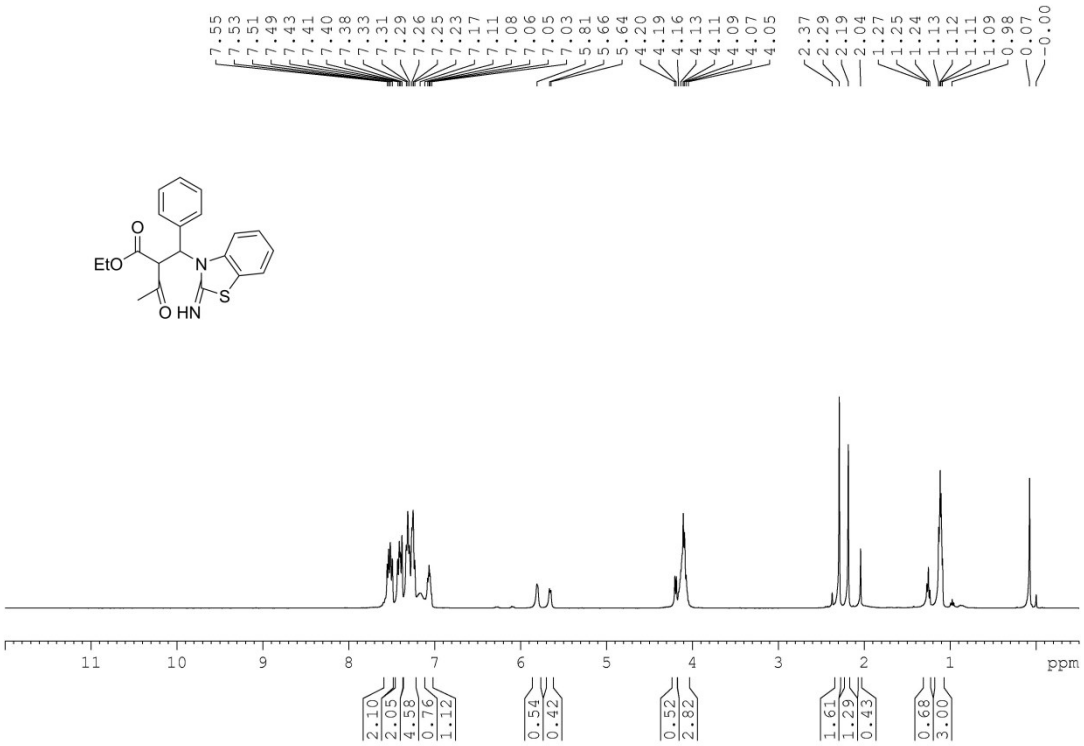

Fig. S32 ^{1}H NMR spectrum of **key intermediate**

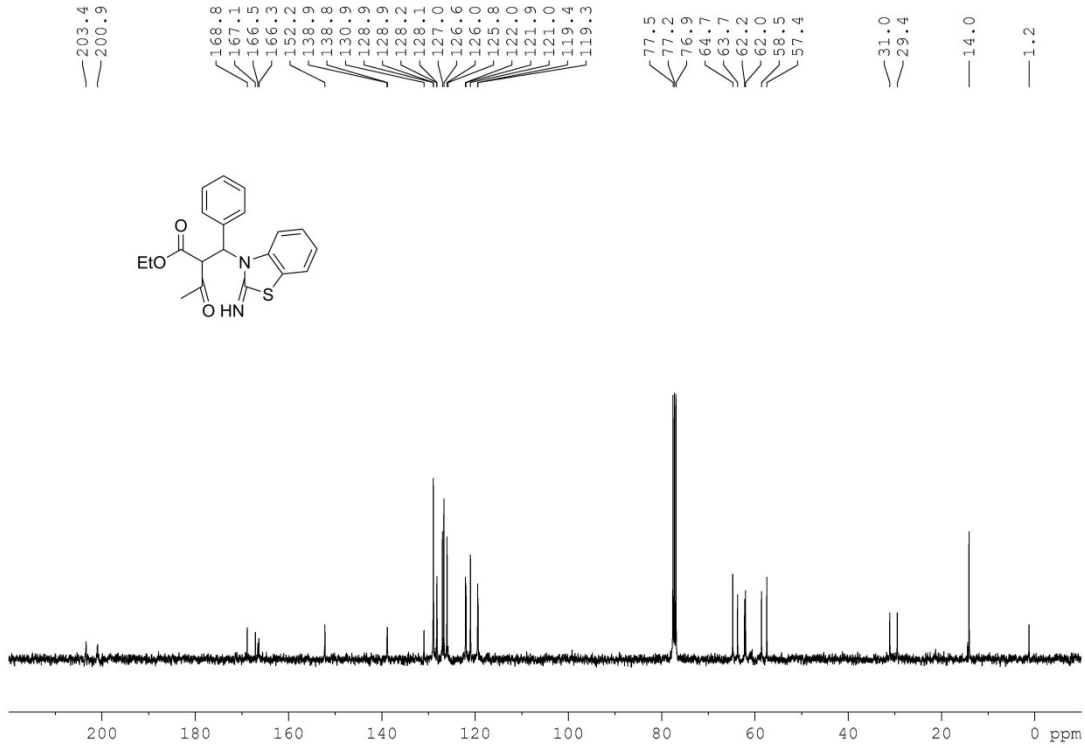

Fig. S33 ^{13}C NMR spectrum of **key intermediate**